The first multi-dimensional Inverse-Scattering-Series internal-multiple-elimination method: a new toolbox option for removing internal multiples that interfere with a primary, without damaging the primary, and without any knowledge of subsurface properties

Yanglei Zou[*]**, Chao Ma**[*] **and Arthur Weglein**[*]

[*]*University of Houston, Department of Physics,*

Houston, Texas, USA, 77204

(May 23, 2018)

GEO-ISS-IME

Running head: **ISS IME**

ABSTRACT

Multiple removal is a long-standing problem in exploration seismology. Many methods have been developed including: stacking, FK filter, Radon transform, deconvolution and Feedback loop. These methods make either statistical assumptions, assume move-out differences, or require knowledge of the subsurface and the generators of the multiples. As the industry trend moved to deep water and more complex on-shore and off-shore geologic plays, these methods often bumped up against their assumptions and had difficulty or failed. As a direct response, the Inverse-Scattering-Series(ISS) algorithms for free surface and internal multiples, made none of these limiting assumptions (Weglein et al. (2003)). There are subseries in the Inverse-Scattering-Series that can achieve different seismic tasks. These

subseries are in terms of data, without requiring any subsurface information. The ISS free surface algorithm (Carvalho (1992), Weglein et al. (1997)) is the only method that predicts the exact time and exact amplitude of every free surface multiple at every offset. The ISS internal multiple algorithm (Araújo et al. (1994),Weglein et al. (1997),Weglein et al. (2003)) predicts the exact time and approximate amplitude of every internal multiple at all offsets. In addition to not requiring any subsurface information, these ISS free surface elimination and internal multiple attenuation algorithms, are model-type independent , that is, they are exactly the same unchanged algorithm for an acoustic, elastic, isotropic, anisotropic and anelastic subsurface.

In principle, a method that removes an internal multiple requires both the correct time and amplitude of the internal multiples at all offsets. Since the ISS internal multiple attenuation algorithm provides the correct time and approximate amplitude, something additional needs to brought in to fill the gap between the predicted and actual internal multiple. There are different ways to fill the gap. There are indirect and direct methods to fill that gap. For indirect methods, the idea is to use a property that data would satisfy if the multiple would be removed compared to when the multiple is present. One idea is that the data without the multiple would have less 'energy' compared to the data with the multiple. That is the idea behind energy minimization adaptive subtraction. In practice, the ISS internal-multiple-attenuation algorithm is usually combined with an energy-minimization adaptive subtraction to remove internal multiples. When internal multiples and primaries are isolated, this combined algorithm can be effective in removing internal multiples. When internal multiples are proximal to and/or interfering with a primary, the criteria of energy-minimization adaptive subtraction can fail. This failure of energy-minimization adaptive subtraction can lead to removing/damaging an interfering target primary, that is the worst

possible outcome. In this work, we provide the first multi-dimensional ISS internal-multiple-elimination algorithm that can predict both the correct time and the correct amplitude of all first-order internal multiples at all offsets. That allows for new algorithm surgically removing internal multiples that interfere with other events/primaries events without damaging e.g. the interfering primary. This elimination algorithm is an important part of the three-pronged strategy proposed by Weglein (2014) :

1. Provide the prerequisites for ISS multiple removal methods for on-shore applications (e.g. removing and predicting the reference wave field and reflection data and to de-ghost the reflection data).

2. Develop internal-multiple elimination algorithms from the ISS.

3. Develop a replacement for the energy-minimization criteria for adaptive subtraction that derives from and always aligns with the ISS elimination algorithm.

The first of the three-pronged strategy have been progressed by Weglein et al. (2002), Zhang (2007), Mayhan and Weglein (2013),Wu and Weglein (2016), Zhang and Weglein (2016),Shen and Weglein (2017). The third is a topic of active research interest. This paper provides an effective response to the second part of the three-pronged strategy. We provide this elimination algorithm as a new capability in the multiple-removal toolbox and a new option for circumstances when this type of capability is called for, indicated and necessary.

INTRODUCTION

The Inverse-Scattering-Series allows all seismic processing objectives, such as free-surface-multiple removal, internal-multiple removal, depth imaging and non-linear parameter estimation to be achieved directly in terms of data, and without any need to estimate or know subsurface properties.Weglein et al. (2003) introduce the concept of isolated task subseries of the ISS to achieve those specific tasks.

For internal-multiple removal, the ISS internal-multiple-attenuation algorithm (Araújo et al. (1994),Weglein et al. (1997) and Weglein et al. (2003)) makes none of the assumptions of other internal-multiple removal methods (e.g. stacking, FK filter, Radon transform, deconvolution and Feedback loop.). It is a part of isolated task specific subseries. The ISS internal-multiple-attenuation algorithm is the most capable internal-multiple removal method today used in industry and the only method that can predict the correct time and approximate and well-understood amplitude for all first-order internal multiples at once, without any subsurface information. It is especially effective when the subsurface is complicated and unknown because of the no requirement of the subsurface information.

Figure 10 shows the requirements and properties of ISS free-surface multiple elimination algorithm compared to SRME (top) and ISS internal multiple attenuation algorithm compared to the internal multiple removal methods from Delft (bottom). For more details, please see Ma et al. (2018)

The two figures below show a field data example for ISS multiple removal methods (free-surface-multiple elimination and internal-multiple attenuation). The data is from the Mississippi Canyon WesternGeco challenge data set. Figure 11 shows the result after applying ISS free-surface-multiple elimination algorithm (Carvalho et al. (1992),Weglein et al.

(1997)). The left panel is a stack of a field data set. The right panel is the result of ISS free-surface multiple removal (Matson et al. (2000),Weglein et al.(2003)). Figure 12 shows the same data after ISS internal multiple attenuation. It shows two common offset panels at 1450ft and 2350ft, respectively. The left part of the common offset panels show the data before internal multiple attenuation. The center panel of the common offset panels show the estimated internal multiples by the ISS internal multiple attenuation algorithm . The right side panel of the common offset panels show the data after internal multiple attenuation. The WesternGeco Mississippi Canyon challenge results were the first marine field data test of the ISS free surface and internal multiple algorithm and were very positive and extremely encouraging (Matson et al. (2000),Weglein et al.(2003)).

When an internal multiple is spatially and temporally separated from other events, the ISS internal-multiple attenuator combined with energy-minimization adaptive subtraction is often successful and effective. When internal multiples are proximal to and/or interfering with other events, e.g. a primary, the criteria of energy-minimization adaptive subtraction can fail (e.g., the energy can increase rather than decrease when an internal multiple is removed from a destructively interfering primary and internal multiple). With interfering events, applying energy-minimization adaptive subtraction can lead to removing/damaging the target primary. Damaging the target primary is the worst possible outcome.

To address this challenging problem, Weglein (2014) proposed a three-pronged strategy:

1. Provide the prerequisites for ISS multiple removal methods for on-shore applications (e.g. removing and predicting the reference wave field and reflection data and to de-ghost the reflection data).

2. Develop internal-multiple elimination algorithms from the ISS.

5

3. Develop a replacement for the energy-minimization criteria for adaptive subtraction that derives from and always aligns with the ISS elimination algorithm.

The first of the three-pronged strategy have been developed by Weglein et al. (2002), Zhang (2007), Mayhan and Weglein (2013). Recent progress in preprocessing non- horizontal undulating off-shore cables and on-shore acquisition can be found in the following references Wu and Weglein (2016), Zhang and Weglein (2016),Shen and Weglein (2017). The third is a topic of active research interest. In discussing the second of the three prongs, that is, the upgrade of the ISS internal multiple attenuator to become an eliminator, we need to begin with a review of the strengths and limitations of the attenuator. The first order ISS internal multiple attenuator always attenuates all internal multiples of first order from all reflectors at once, directly and without subsurface information, automatically and without interpretive intervention. That is a tremendous strength, and is a constant and holds independent of the circumstances and complexity of the geology and the play. The primaries in the reflection data that enter the algorithm provides that delivery, without our requiring the primaries to be identified or in any way separated. The other events in the reflection data, that is, the internal multiples, when they enter the first order ISS internal multiple algorithm will alter and prep the higher order internal multiples and thereby assist and cooperate with higher order ISS internal multiple attenuation terms, to attenuate higher order internal multiples. That is a benefit and definite asset, and its always in action and completely automatic. However, there is a downside, a limitation. There are cases and certain well-defined circumstances when internal multiples that enter the first order attenuator can predict spurious or false events. The circumstances typically involve a large number of internal multiple generators. That is a well-understood shortcoming of the leading order term, when taken in isolation, but is not an issue for the entire ISS internal

multiple capability. That shortcoming of the first order ISS attenuator is anticipated by the ISS and higher order ISS internal multiple terms exist to precisely remove that issue of spurious event prediction, and taken together with the first order term, no longer experiences spurious event prediction. Chao Ma and Hong Liang provided those higher-order terms and tests with complex multiple generators show the effectiveness of their spurious removal higher order ISS internal multiple attenuation algorithms (Ma et al. (2012) , H. Liang and Weglein (2012) and Ma and Weglein (2014)).

In a similar way, there are higher order ISS internal-multiple removal terms that provide the capability to eliminate internal multiples, i.e. predict correct time and amplitude of internal multiples, when taken together with the current leading-order ISS internal multiple attenuation term. The initial idea is provided by Weglein and Matson (1998) in which the attenuation factor (a collection of extra transmission coefficients and the difference between attenuation and elimination) is systematically studied. There are further discussions in Ramírez (2007). Herrera and Weglein (2012) proposed an internal-multiple elimination algorithm for all first-order internal multiples generated at the first reflector for 1D normal incidence. A first order internal multiple has one downward reflection in its history. That downward reflection can occur at any reflector. Benefiting from the previous work, Zou and Weglein (2014) proposed a general ISS internal-multiple-elimination algorithm for a 1D earth for internal multiples generated by ALL reflectors at once. In this paper, we propose the first multi-dimensional ISS internal-multiple elimination method that can eliminate internal multiples interfering with a primary, without subsurface information, and without damaging the primary. In the development of elimination algorithm in this paper, we assumed an acoustic relationship $T = 1 + R$ between transmission coefficients T and reflection coefficients R, without needing to know, estimate or determine either. In this

paper, we provide numerical tests and analysis for a 2D model. The results demonstrate that the elimination algorithm can predict both the accurate amplitude and arrival time of first-order internal multiples. We also compare the ISS elimination result with attenuation plus energy-minimization adaptive subtraction. The comparison shows that the ISS internal-multiple-elimination algorithm is more effective and more compute-intensive than the current most capable ISS attenuation-plus-adaptive-subtraction method. We provide this elimination algorithm as a new capability in the multiple-removal toolbox and a new option for circumstances when this type of capability is called for, indicated and necessary. In the future, we will develop a model-type independent internal-multiple elimination algorithm that can accommodate an elastic and inelastic subsurface. There are other related work including Fu et al. (2018) which studied and tested the ISS elimination algorithm in an absorptive medium and reported encouraging result.Innanen (2017) have investigated the sensitivity of the choice of epsilon in the ISS internal attenuator equation in terms of the required lower higher lower pseudo depth relation that the subevents need to satisfy in order to combine to predict an internal multiple. They have suggested and have exemplified a non-stationary epsilon strategy, that navigate the issues between a too small (predictor becomes a primary-like artifact) and too large (missing predicting some internal multiples) epsilon value, and they propose that a priori geologic information can assist. Our view is that the very meaning of a primary and an internal multiple is a bandwidth dependent concept, and hence , e.g., there are events that we consider to be primaries that in fact under broader bandwidth would be superposition of sub-resolution internal multiples. The ISS internal multiple attenuation and elimination algorithms assume definitions of primaries and internal multiples that are defined and have meaning within the bandwidth of the recorded data set.

THE ISS INTERNAL-MULTIPLE ATTENUATION ALGORITHM AND THE DIFFERENCE BETWEEN ATTENUATION AND ELIMINATION

The ISS internal-multiple attenuation algorithm is first given by Araújo et al. (1994) and Weglein et al. (1997). The 1D normal incidence version of that algorithm for a normal incident plane wave is presented below (The 2D version is given in Araújo et al. (1994),Weglein et al. (1997) and Weglein et al. (2003) and the 3D version is a straightforward extension.),

$$b_3(k) = \int_{-\infty}^{\infty} dz e^{ikz} b_1(z) \int_{-\infty}^{z-\varepsilon_2} dz' e^{-ikz'} b_1(z') \int_{z'+\varepsilon_1}^{\infty} dz'' e^{ikz''} b_1(z''). \tag{1}$$

In equation (1) $b_1(z)$ is the constant velocity Stolt migration of the data of a 1D normal incidence spike plane wave. ε_1 and ε_2 are two small positive numbers introduced to define a "lower-higher-lower" relationship amongst the three integrals. $b_3(k)$ is the predicted internal multiples in the vertical wavenumber domain. This algorithm can predict the correct time and approximate amplitude of all first-order internal multiples at once without any subsurface information.

The ISS internal-multiple attenuation algorithm automatically combines three primaries in the data to predict a first-order internal multiple. In Weglein et al.(2003), this algorithm is proved to be model type independent, that is, it is one exactly unchanged algorithm independent of the assumed model type of the subsurface (acoustic, elastic, anisotropic, anelastic). The prediction has extra transmission coefficients (also called attenuation factor) (figure 13 and figure 14) compared with the actual internal multiple. For the first-order internal multiple generated at the shallowest reflector (figure 13) the extra transmission coefficients are - $T_{01}T_{10}$. All first-order internal multiples generated at the shallowest

reflector have the same attenuation factor.

In the ISS internal multiple attenuation algorithm prediction, the attenuation factor for an internal multiple generated (For first-order internal-multiple we consider the location of the reflector where the single downward reflection occurs as the multiple generator.) by the jth reflector, AF_j, is given by the following:

$$AF_j = \begin{cases} T_{0,1}T_{1,0} & (for\ j = 1) \\ \prod_{i=1}^{j-1}(T_{i-1,i}^2 T_{i,i-1}^2)T_{j,j-1}T_{j-1,j} & (for\ 1 < j < J) \end{cases} \quad (2)$$

The interfaces are numbered starting with the shallowest location labeled as 1,2 3, ..., J. The attenuation factor is a collection of extra transmission coefficients at and above the generator and is the difference between attenuation and elimination. The subscript j represents the generating reflector, and J is the total number of interfaces in the model. In the equation, $\prod(T_{i-1,i}^2 T_{i,i-1}^2)$ corresponds to the transmission coefficients related to the reflectors from the shallowest down to but not including the generator, $T_{j,j-1}T_{j-1,j}$ corresponds to the extra transmission coefficients related to the generator.

INTERNAL MULTIPLE ELIMINATION ALGORITHM AMPLITUDE ANALYSIS

Weglein and Matson (1998), Weglein et al.(2003), Ramírez (2007) and Herrera and Weglein (2012) studied the attenuation factor and provided the initial idea for elimination, that is, to remove the attenuation factor(the difference between attenuation and elimination) in terms of higher orders of reflection data, from the Inverse-Scattering Series. For internal multiples generated by the shallowest reflector, the difference between attenuation and elimination is AF_1 . To remove AF_1 in the prediction, we have

$$elimination = \frac{attenuation}{AF_1} \tag{3}$$

$$= \frac{attenuation}{T_{0,1}T_{1,0}}$$

$$= \frac{attenuation}{1 - R_1^2}$$

$$= attenuation + attenuation \times R_1^2 + attenuation \times R_1^4 + ...$$

where the first term is the attenuation algorithm, the term $attenuation \times R_1^2$ corresponds to the first higher order term towards elimination and the next term are beyond the first higher order term towards elimination.

Figure 15 shows a diagram for the attenuation algorithm where three subevents that satisfy a higher-lower-higher relationship are combined to predict an internal multiple. The predicted multiple has the correct time and approximate amplitude. The difference between attenuation and elimination is the attenuation factor (equation 2), which is a set of transmission coefficients. The attenuation factor depends on the shallowest reflector down to the generator of the internal multiple. The generator of the internal multiple is defined as the reflector where the internal multiple has its shallowest downward reflection. In the ISS internal multiple attenuation algorithm the subevent in the middle integral contains the transmission coefficients from the shallowest reflector down to the generator of the internal multiple. Therefore, the higher order elimination terms has more orders of data in the middle integral instead of the two outer integrals. These higher orders of data only change the amplitude of the prediction. Figure 16 shows a diagram for a higher order term in the elimination algorithm. There are two more orders of data in the middle integral compared to the attenuation algorithm. These two higher orders of data provides R_1^2 in the prediction (second terms in equation (3)). Similarly, there are other higher order terms (e.g. Figure

17) that corresponds to other higher order terms in equation (3).

For internal multiples generated by all the reflectors, the difference between attenuation and elimination is AF_j(equation (2)) . To remove AF_j in the prediction, in terms of higher orders of data, Zou and Weglein (2014), Zou et al. (2016) provide an expansion,

$$
\begin{aligned}
elimination = & \frac{attenuation}{AF_i} \\
= & \frac{attenuation}{(1 - R_i^2)(1 - R_1^2 - R_2'R_2 - \cdots - R_{i-1}'R_{i-1})^2} \\
= & attenuation(1 + R_i^2 + R_i^4 + \cdots)(1 + (R_1^2 + R_2R_2' + \cdots + R_{i-1}R_{i-1}') + \cdots)^2 \\
= & attenuation(1 + R_i^2 + R_i^4 + \cdots + (R_1^2 + R_2R_2' + \cdots + R_{i-1}R_{i-1}') + \cdots) \\
= & attenuation + attenuation \times R_i'^2 + attenuation \times R_i'^4 + \cdots \\
& + attenuation \times (R_1^2 + R_2R_2' + \cdots + R_{i-1}R_{i-1}') + \cdots
\end{aligned}
\tag{4}
$$

Each term in this expansion corresponds to a higher order term in the Inverse Scattering Series (A more detailed discussion is found in later sections).

1D NORMAL INCIDENCE ISS INTERNAL-MULTIPLE ELIMINATION ALGORITHM

In Weglein et al.(2003), it has been demonstrated that there are sub-series inside the Inverse-Scattering-Series that can achieve different seismic tasks in terms of only data and reference information (assumed as a homogeneous whole space). For internal multiple removal, b_1 is the data migrated with the reference velocity. Thus there must exist an internal multiple elimination sub-series in terms of only the data where the ISS internal multiple attenuation algorithm is the first term in the sub-series.

A first-order internal multiple has one downward reflection in its history. The subevents in the outer integrals contains information both above and below the generator. The discussion in the previous section demonstrates that in the ISS internal multiple attenuation algorithm prediction, all first-order internal multiples generated at the same reflector have the same attenuation factor. Internal multiples generated at different reflectors have different attenuation factors. We also derived a general formula for the attenuation factor for all reflectors. The attenuation factor contains all transmission coefficients from the shallowest reflector down to the reflector generating the multiple. The subevent in the middle integral of ISS internal multiple attenuation algorithm contains all those transmission coefficients. Therefore, by modifying the middle integral (adding higher orders of data(b_1) in the middle integral), the attenuation factor can be removed and the attenuation algorithm turns into an elimination algorithm, that is, from

$$b_3^{IM}(k) = \int_{-\infty}^{\infty} dz e^{ikz} b_1(z) \int_{-\infty}^{z-\varepsilon_2} dz' e^{-ikz'} b_1(z') \int_{z'+\varepsilon_1}^{\infty} dz'' e^{ikz''} b_1(z'') \tag{5}$$

to

$$b_E^{IM}(k) = \int_{-\infty}^{\infty} dz e^{ikz} b_1(z) \int_{-\infty}^{z-\varepsilon_2} dz' e^{-ikz'} F[b_1(z')] \int_{z'+\varepsilon_1}^{\infty} dz'' e^{ikz''} b_1(z'') \qquad (6)$$

The latter is the closed form of the elimination sub-series (The details of $F[b_1(z)]$ will be discussed later.). To remove all attenuation factors in the prediction, the $F[b_1(z)]$ should have the following form (Each primary sub-event in the middle integral is used to predict internal multiples generated by the corresponding reflector, e. g., the first primary sub-event is used to predict the multiples generated by the first reflector, the second primary sub-event is used to predict the multiples generated by the second reflector, and so on. Therefore, in the elimination algorithm, each amplitude sub-event in the middle integral should be divided by the corresponding attenuation factor, so that in the prediction, the attenuation factor originally appears in the attenuation algorithm can be canceled, that is, predicting the correct amplitude.):

$$\begin{aligned} F[b_1(z')] =& \frac{R_1}{AF_{j=1}}\delta(z' - z_1) + \frac{R'_2}{AF_{j=2}}\delta(z' - z_2) + \cdots + \frac{R'_n}{AF_{j=n}}\delta(z' - z_n) + \cdots \\ =& \frac{R_1}{1 - R_1^2}\delta(z' - z_1) + \frac{R'_2}{(1 - R_1^2)^2(1 - R_2^2)}\delta(z' - z_2) + \cdots \\ &+ \frac{R'_n}{(1 - R_1^2)^2(1 - R_2^2)^2 \cdots (1 - R_{n-1}^2)^2(1 - R_n^2)}\delta(z' - z_n) + \cdots \qquad (7) \end{aligned}$$

Here we used the relationship T=1+R between transmission coefficient T and reflection coefficient R. This relationship is valid only in an acoustic medium. It is an approximation for an elastic medium. In appendix A, we have more detailed discussion on this topic.

By introducing an intermediate function called g(z) in which the amplitude of each event corresponds to a reflection coefficient, we find a way to construct $F[b_1(z)]$ by using data $(b_1(z))$ and g(z). After that, we find an integral equation about $b_1(z)$ and g(z). Solving the latter equation for g(z) and integrate it into the first part, $F[b_1z]$ can be obtained.(shown

14

in figure 5).

By using this strategy, the $F[b_1(z)]$ is (See appendix B for the derivation):

$$F[b_1(z)] = \frac{b_1(z)}{[1 - (\int_{z-\varepsilon}^{z+\varepsilon} dz' g(z'))^2][1 - \int_{-\infty}^{z-\varepsilon} dz' b_1(z') \int_{z'-\varepsilon}^{z'+\varepsilon} dz'' g(z'')]^2}$$

(8)

$$g(z) = \frac{b_1(z)}{1 - \int_{-\infty}^{z-\varepsilon} dz' b_1(z') \int_{z'-\varepsilon}^{z'+\varepsilon} dz'' g(z'')}$$

(9)

To derive the $F[b_1(z)]$ from $b_1(z)$, g(z) must first be solved in equation (9). Thereafter, g(z) is integrated into equation (8).

1D PRE-STACK ISS INTERNAL-MULTIPLE ELIMINATION ALGORITHM

In appendix D, we discussed a pre-stack two-reflector analytic example and derived the attenuation factor for a 1D pre-stack model. The 1D pre-stack attenuation factor has the same structure as the 1D normal incidence attenuation factor except the transmission coefficients are angle dependent. The 1D pre-stack ISS internal multiple elimination algorithm is developed in a similar way to the 1D normal incidence algorithm. The differences between the 1D pre-stack algorithm and the 1D normal incidence algorithm are that the 1D pre-stack algorithm has one more variable k, and the 1D pre-stack algorithm accommodates the angle dependent reflection coefficients. The following equations are the 1D pre-stack ISS internal multiple elimination algorithm.

$$b_E^{IM}(k, 2q) = \int_{-\infty}^{\infty} dz e^{2iqz} b_1(k, z) \int_{-\infty}^{z-\varepsilon_1} dz' e^{-2iqz'} F[b_1(k, z')] \int_{z'+\varepsilon_2}^{\infty} dz'' e^{2iqz''} b_1(k, z'') \quad (10)$$

$$F[b_1(k, z)] = \frac{1}{2\pi} \int_{-\infty}^{\infty} \int_{-\infty}^{\infty} dz' dq'$$

$$\times \frac{e^{-iq'z} e^{iq'z'} b_1(k, z')}{[1 - \int_{-\infty}^{z'-\varepsilon} dz'' b_1(k, z'') e^{iq'z''} \int_{z''-\varepsilon}^{z''+\varepsilon} dz''' g^*(k, z''') e^{-iq'z'''}]^2 [1 - |\int_{z'-\varepsilon}^{z'+\varepsilon} dz'' g(k, z'') e^{iq'z''}|^2]}$$

$$(11)$$

$$g(k, z) = \frac{1}{2\pi} \int_{-\infty}^{\infty} \int_{-\infty}^{\infty} dz' dq' \frac{e^{-iq'z} e^{iq'z'} b_1(k, z')}{1 - \int_{-\infty}^{z'-\varepsilon} dz'' b_1(k, z'') e^{iq'z''} \int_{z''-\varepsilon}^{z''+\varepsilon} dz''' g^*(k, z''') e^{-iq'z'''}} \quad (12)$$

A NUMERICAL TEST FOR 1D PRE-STACK SYNTHETIC ELASTIC PP DATA

We test the 1D pre-stack internal-multiple elimination algorithm for an four-reflector elastic model shown in figure 6. Figure 7 shows the PP data generated from this model by reflectivity method. Figure 8 and figure 9 show a section (2.8s-3.1s) of the data and attenuation and elimination prediction results.

The left picture in figure 8 shows a section in the input data. In this section ,there are 3 major events interfering with each other: a converted P primary, an internal multiple generated from the first reflector and another internal multiple generated from the third reflector. The middle picture in figure 8 shows the attenuation algorithm predicted internal multiples, it clearly shows the predicted internal multiples have correct time and approximate amplitude. The right picture in figure 8 shows the elimination algorithm prediction, the time is correct and the amplitude is more accurate. The left picture in figure 9 shows the primaries in the data. (Because it is a synthetic test, we can generate only the primaries and use them as a benchmark.) The middle picture in figure 9 shows the result by subtracting the attenuation algorithm prediction from the data. The internal multiples has been reduced, but there still remains residues. The right picture in figure 9 shows the result by subtracting the elimination algorithm prediction from the data. We can see that the multiples has been removed and the primary is recovered. (Note that there is some small residual due to: (1) the inaccuracy of the numerical Hankel transform and (2) the assumption of an acoustic relationship between transmission coefficients and reflection coefficients. The Hankel transform is used here because the earth is assumed to be 1D and the data is generated by a 3D source. The input is data recorded by a line of receivers along a

radius within a cylindrical coordinate system and that gives rise to the Hankel transform. If we had a full area coverage of receivers, we can use a Fast Fourier Transform instead of numerical Hankel transform and that will remove the residue due to the numerical Hankel transform. The residue due to the acoustic relationship assumption between transmission and reflection coefficients will be addressed in the future when the elimination method is extended to elastic/anelastic media)

THE FIRST INVERSE-SCATTERING-SERIES INTERNAL-MULTIPLE ELIMINATION METHOD FOR A MULTI-DIMENSIONAL SUBSURFACE

The inverse scattering series(ISS) allows for all processing objectives to be achieved through isolated task ISS subseries that input the recorded reflection data and a homogeneous reference Green's function, G_0(see e.g. Weglein et al. (2003)). For the 1D and multi-D internal multiple attenuation algorithms (Araújo et al. (1994),Weglein et al. (1997) and Weglein et al. (2003)), the input $b_1(k_g, k_s, z)$ is a combination of data and a water speed Green's function. The input, $b_1(k_g, k_s, z)$ is a source side obliquity factor $-2iq_s$ times a Stolt CIII water speed migration. The role of the obliquity factor, $-2iq_s$, is to make the reference wave a localized plane wave in every dimension. That in turn facilitates events in all dimensions to become local-a useful property for the internal multiple attenuation algorithm. The 1D internal multiple elimination algorithm(Zou and Weglein (2014)) fills the gap between attenuating and eliminating internal multiples from a 1D subsurface with higher order terms in the one-D version of the 2D $b_1(k_g, k_s, z)$. That is $b_1(k, z)$, where $k_g = k_s = k$ for a 1D subsurface. The quantity,$b_1(k_g, k_s, z)$ contains the multi-D generalization and extension of the specular plane wave reflection coefficient and has its basis in a point scattering, point

reflectivity model or scattering operator, V_1 (in e.g. Weglein et al. (2003) and Stolt and Weglein (2013)). That general operator can accommodate specular and non-specular scattering(curved reflectors and diffractors(pinch-outs)). The derivation of the multi-D internal multiple attenuation algorithm from a part of the third term $G_0 V_1 G_0 V_1 G_0 V_1 G_0$ in the inverse scattering series provides the template and guide for deducing the multidimensional elimination algorithm.

In addition to being directly derivable by collecting all the W shape and self-interactions diagrams(see figure15,16 and 17, these self-hits fix the amplitude issue of the leading-order term) in the ISS. The multi-D internal multiple eliminator is also recognized as the simplest multi-D generalization of the one-D eliminator. That's a reasonable requirement for a multi-D internal multiple eliminator to satisfy. The 1D eliminator benefits from an analytic expression of the gap filling needed between attenuate and eliminate and how that gap is provided in terms of a 1D Stolt CIII water speed migration $b_1(k, z)$. The multi-D gap filling ISS internal multiple eliminator is directly deduced from the ISS without the benefit of knowing the underlying detailed cause and contribution to the gap, as is available in 1D (please see the sections on 1D in previous pages.).

That analysis produces the 2D or 3D internal multiple elimination algorithm. Below we show the 2D form of the elimination algorithm

$$b_E(k_s, k_g, q_g + q_s) =$$

$$\int\limits_{-\infty}^{+\infty}\int\limits_{-\infty}^{+\infty} dk_1 dk_2 \int\limits_{-\infty}^{+\infty} dz_1 b_1(k_g, k_1, z_1) e^{i(q_g+q_1)z_1}$$

$$\times \int\limits_{-\infty}^{z_1-\varepsilon} dz_2 F(k_1, k_2, z_2) e^{-i(q_1+q_2)z_2} \int\limits_{z_2+\varepsilon}^{+\infty} dz_3 b_1(k_2, k_s, z_3) e^{i(q_2+q_s)z_3} \tag{13}$$

where

$$F(k_1, k_2, z) =$$

$$\int\limits_{-\infty}^{+\infty} d(q_1+q_2) e^{-i(q_1+q_2)z} \int\limits_{-\infty}^{+\infty}\int\limits_{-\infty}^{+\infty} dk' dk'' \int\limits_{-\infty}^{+\infty} dz' b_1(k_1, k', z') e^{i(q_1+q')z'}$$

$$\times \int\limits_{-\infty}^{z'-\varepsilon} dz'' b_1(k', k'', z'') e^{-i(q'+q'')z''} \int\limits_{z''-\varepsilon}^{z''+\varepsilon} dz''' g(k'', k_2, z''') e^{i(q''+q_2)z'''} \tag{14}$$

and

$$g(k_1, k_2, z) =$$

$$\int\limits_{-\infty}^{+\infty} d(q_1+q_2) e^{-i(q_1+q_2)z} \int\limits_{-\infty}^{+\infty}\int\limits_{-\infty}^{+\infty} dk' dk'' \int\limits_{-\infty}^{+\infty} dz' b_1(k_1, k', z') e^{i(q_1+q')z'}$$

$$\times \int\limits_{-\infty}^{z'-\varepsilon} dz'' b_1(k', k'', z'') e^{-i(q'+q'')z''} \int\limits_{z''-\varepsilon}^{z''+\varepsilon} dz''' g(k'', k_2, z''') e^{i(q''+q_2)z'''} \tag{15}$$

where $F(k_1, k_2, z)$ and $g(k_1, k_2, z)$ are (as in the 1D case) two intermediate functions.

At this point we review and summarize the data processing steps for towed streamer data. The recorded wavefield $D(x_s, x_g, t)$ first removes the reference wavefield, the ghosts and the free surface multiples. After those steps we have $D'(x_s, x_g, t)$ which contains only primaries and internal multiples. Next $b_1 + b_3$ denotes the ISS internal multiple attenuation algorithm, $b_1 + b_{3E}$ denotes the ISS internal multiple elimination algorithm. Finally, we obtain the $D''(x_s, x_g, t)$ which contains only primaries.

$D(x_g,x_s,t)$	the recorded wavefield
$D'(x_g,x_s,t)$	recorded wavefield with removal of (1) reference wave field, (2) source and receiver ghost and (3) free surface multiples
Then D' is water speed migrated and multiplied by $-2iq_s$, producing b_1	
$b_1 + b_3$	first order internal multiples attenuated
$b_1 + b_E$	first order internal multiples eliminated
$b_1 + b_E = -2iq_s D''$	D'' is the data contains only primaries

Figure 1: Steps that towed streamer data goes through (in 2D, it's similar in 3D) in the removal of free surface and internal multiples. D, D' and D" are the recorded data, data with free surface multiples removed and data without free surface and internal multiples, respectively.

2D SYNTHETIC DATA EXAMPLE

Figure 18 shows the 2D model, the data is generated by finite difference method. There is a salt dome structure in the middle of the model. The shape is designed so that the primary generated by the lower boundary of the salt dome is negatively interfering with an internal multiple. In this synthetic data, there are 127 shot gathers, each shot gather contains 127 receivers. The source and receiver interval is 30 meters and time interval is 0.002s.

In order to see the result more clearly, we show the zero offset traces results. Figure 19 shows the zero offset traces of the input data. Compared to the model, we can see clearly

that the lower boundary of the salt dome is almost invisible because the primary generated by the lower boundary of the salt dome is negatively interfere with an internal multiple. Figure 20 shows the zero offset traces results after ISS internal-multiple attenuation and adaptive subtraction. We can see the lower boundary of the salt dome is still not visible. It is because the criteria of the energy minimization adaptive subtraction fails, that is, the primary energy after subtraction is larger than the interfering events. Figure 21 shows the 0-offset-trace result after internal-multiple elimination. The lower boundary of the salt dome is recovered in the result. It demonstrates that the elimination algorithm can predict both correct time and amplitude and can eliminate internal multiples without touching the primary

Next we show two numerical examples where primaries and internal multiples interfere with each other. We choose a 1D prestack example to test because wave-theoretic (not ray-theory) based modeling can only produce a data set exclusively with primaries when the subsurface is 1D acoustic or 1D elastic.

Figure 22 shows the 1D model that mimics the 2D model. Figure 23 shows the synthetic data generated based on the 1D model. Notice that, only three primaries (P_1, P_2, and P_3) and one first-order internal multiple generated by the first two reflectors (IM_{212}) are considered. P_3 and IM_{212} destructively interfere at offset around 1000 m.

Figures 24 and 25 show the predictions of internal multiples by the ISS IMA and IME, respectively. The predicted internal multiple (IM_{212}) have the same time which agrees with the actual internal multiple in the data. The amplitude of these two internal multiple predictions are different, as expected. The prediction result from the attenuation algorithm has an approximate amplitude (compared with the actual internal multiple in the data)

whereas the prediction result from the elimination algorithm has an accurate amplitude.

Figures 26, 27 and 28 show the wiggle plots of P_3 and IM_{212}, P_3 and IM_{212} in the data, respectively. Figure 29 shows the result after directly subtracting the prediction result of ISS IMA from the data. Comparing Figure 26 and 29, we notice that, (1) at the place where primary and internal multiple destructively interfere (highlighted in blue circle in Figure 29), primary is partially recovered, and (2) at the place where primary and internal multiple do not interfere (highlighted in red circle in Figure 29), internal multiple residues are left.

Figure 30 shows the result of ISS IMA plus energy-minimization adaptive subtraction. We use a single-channel matching filter for the adaptive subtraction process and the subtraction operator is calculated assuming that the predicted multiple only has a scalar difference with the actual multiple (Equation (2) and (3) in Wang (2003)). Comparing figure 30 with figure 26 and 29, we find that the at the place where primary and internal multiple do not interfere, energy-minimization adaptive subtraction help to remove the internal multiple residue left by the ISS IMA, however, the adaptive subtraction step can harm the partially recovered primary by ISS IMA. Figure 31 show the result after directly subtracting the prediction result of ISS IME from the data. Comparing this result from ISS IME (Figure 31) with the result from ISS IMA with (Figure 30) and without (Figure 29) energy-minimization adaptive subtraction, we notice that, (1) with this amplitude improved prediction from ISS IME, the internal multiple in the data can be effectively removed (no residues left compared the result from ISS IMA), and (2) without using energy-minimization adaptive subtraction, the primary can be recovered without damage from the adaptive step.

CONCLUSION

The ISS multi-dimensional internal-multiple-elimination algorithm that removes internal multiples is one part of the three-pronged strategy that is a direct response to the current seismic processing and interpretation challenge (elimination of internal multiples proximal to and/or interfering with primaries without damaging the primary). This elimination algorithm addresses the shortcomings of the current most capable internal-multiple-removal method (ISS internal-multiple-attenuation algorithm plus adaptive subtraction). The ISS internal multiple elimination algorithm retains the stand-alone benefits of the ISS internal-multiple-attenuation algorithm in that it can predict all internal multiples from all reflectors at once and without requiring any subsurface information (in contrast to feedback methods that require knowledge of the reflector generators and stripping methods that remove multiples layer by layer and require subsurface information). This ISS internal-multiple-elimination algorithm has demonstrated both effectiveness and more compute-intensiveness in synthetic data tests than the internal-multiple-attenuation method. We provide this new multi-dimensional internal-multiple-elimination method as a new internal-multiple-removal capability in the multiple-removal toolbox. It can remove internal multiples that interfere with primaries without subsurface information and without damaging the primary. A three-pronged strategy(Weglein (2014)) was proposed to address open issues in the removal of internal multiples in complex off-shore and on-shore plays,

1. Provide the prerequisites for ISS multiple removal methods for on-shore applications (e.g. removing and predicting the reference wave field and reflection data and to de-ghost the reflection data).

2. Develop internal-multiple elimination algorithms from the ISS.

3. Develop a replacement for the energy-minimization criteria for adaptive subtraction that derives from and always aligns with the ISS elimination algorithm.

Our plans include developing an alternative adaptive-subtraction criteria for internal-multiple elimination derived from, and always aligned with the ISS elimination algorithm. That would be analogous to the new adaptive criteria for free-surface-multiple removal proposed by Weglein (2012), as a replacement for the energy-minimization criteria for adaptive subtraction.

APPENDIX A ATTENUATION FACTOR IN ACOUSTIC AND ELASTIC MEDIUM

The ISS internal-multiple elimination algorithm is developed based on the relationship T=1+R between reflection coefficients and transmission coefficients. The relationship of T=1+R does not hold strictly for elastic medium due to converted waves. The following figure 2 shows the attenuation factor for an acoustic two reflector model and an elastic two reflector model. For the acoustic model, above the reflector $V = 1500m/s$, $\rho = 1.0 \times 10^3 m^3/kg$, below the reflector $V = 2000m/s$, $\rho = 2.0 \times 10^3 m^3/kg$. For the elastic model, above the reflector $V_p = 1500m/s$, $V_s = 500m/s$, $\rho = 1.0 \times 10^3 m^3/kg$, below the reflector $V_p = 2000m/s$, $V_s = 700m/s$, $\rho = 2.0 \times 10^3 m^3/kg$. The figures shows the attenuation factor for acoustic and elastic medium are close especially for small incident angles.
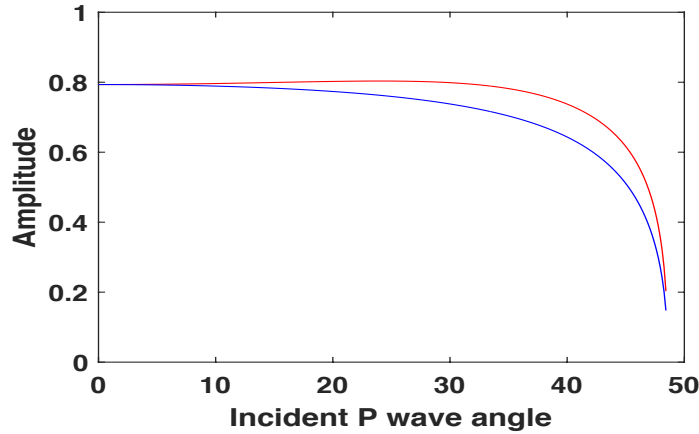
Figure 2: Acoustic and elastic attenuation factor, red line is the attenuation factor for acoustic medium, blue line is the attenuation factor for elastic medium (The amplitude does not have units.)

APPENDIX B DERIVATION OF THE ALGORITHM FOR THE ELIMINATION OF ALL FIRST-ORDER INTERNAL MULTIPLES FROM ALL REFLECTORS IN A 1D MEDIUM

The middle part of the 1D normal incidence algorithm is:

$$F[b_1(z)] = \frac{b_1(z)}{[1 - (\int_{z-\varepsilon}^{z+\varepsilon} dz' g(z'))^2][1 - \int_{-\infty}^{z-\varepsilon} dz' b_1(z') \int_{z'-\varepsilon}^{z'+\varepsilon} dz'' g(z'')]^2} \tag{A-1}$$

$$g(z) = \frac{b_1(z)}{1 - \int_{-\infty}^{z-\varepsilon} dz' b_1(z') \int_{z'-\varepsilon}^{z'+\varepsilon} dz'' g(z'')} \tag{A-2}$$

($\int_{z-\varepsilon}^{z+\varepsilon} dz'' g(z'')$ is a function of z)

Next we will take an analytic 1D normal incidence example to show A-1 and A-2 provide the needed $F[b_1(z)]$ in equation (7). Consider a data with n primaries (For simplicity, here we consider primaries only in the data. The multiples can be accommodated by the ISS comprehensive attenuation/elimination algorithm, Ma et. al (2014)), we have

$$b_1(z) = R_1\delta(z - z_1) + R_2'\delta(z - z_2) + R_3'\delta(z - z_3) + \cdots + R_n'\delta(z - z_n) + \cdots \tag{A-3}$$

$g(z)$ should be

$$g(z) = R_1\delta(z - z_1) + R_2\delta(z - z_2) + R_3\delta(z - z_3) + \cdots + R_n\delta(z - z_n) + \cdots \tag{A-4}$$

Here $b_1(z)$ is known, $g(z)$ is unknown, in the algorithm, $g(z)$ is calculate by $b_1(z)$.

Next we will show that A-1 and A-2 provide the F function $F[b_1(z)]$ in equation (7).

First calculate $\int_{z-\varepsilon}^{z+\varepsilon} dz'' g(z'')$ in both A-1 and A-2:

$$\int_{z-\varepsilon}^{z+\varepsilon} dz'' g(z'') = \int_{z-\varepsilon}^{z+\varepsilon} dz'' [R_1 \delta(z'' - z_1) + R_2 \delta(z'' - z_2) + \cdots + R_n \delta(z'' - z_n) + \cdots]$$

$$= \int_{-\infty}^{\infty} dz'' [R_1 \delta(z'' - z_1) + R_2 \delta(z'' - z_2) + \cdots + R_n \delta(z'' - z_n) + \cdots]$$

$$\times H(z'' - (z - \varepsilon)) H((z + \varepsilon) - z'')$$

$$= R_1 H(z_1 - (z - \varepsilon)) H((z + \varepsilon) - z_1) + R_2 H(z_2 - (z - \varepsilon)) H((z + \varepsilon) - z_2)$$

$$+ \cdots + R_n H(z_n - (z - \varepsilon)) H((z + \varepsilon) - z_n) + \cdots$$

$$= R_1 H((z_1 + \varepsilon) - z) H(z - (z_1 - \varepsilon)) + R_2 H((z_2 + \varepsilon) - z) H(z - (z_2 - \varepsilon))$$

$$+ \cdots + R_n H((z_n + \varepsilon) - z) H(z - (z_n - \varepsilon)) + \cdots \qquad \text{(A-5)}$$

Second calculate $(\int_{z-\varepsilon}^{z+\varepsilon} dz'' g(z''))^2$ in A-1.

$$\left(\int_{z-\varepsilon}^{z+\varepsilon} dz'' g(z'') \right)^2$$

$$= R_1^2 H((z_1 + \varepsilon) - z) H(z - (z_1 - \varepsilon)) + R_2^2 H((z_2 + \varepsilon) - z) H(z - (z_2 - \varepsilon))$$

$$+ \cdots + R_n^2 H((z_n + \varepsilon) - z) H(z - (z_n - \varepsilon)) + \cdots \qquad \text{(A-6)}$$

Then calculate $b_1(z') \int_{z'-\varepsilon}^{z'+\varepsilon} dz'' g(z'')$ in A-1 and A-2.

$$b_1(z') \int_{z'-\varepsilon}^{z'+\varepsilon} dz'' g(z'')$$

$$= R_1^2 \delta(z' - z_1) + R_2 R_2' \delta(z' - z_2) + R_3 R_3' \delta(z' - z_3) + \cdots + R_n R_n' \delta(z' - z_n) + \cdots \qquad \text{(A-7)}$$

$$\int_{-\infty}^{z-\varepsilon} dz' b_1(z') \int_{z'-\varepsilon}^{z'+\varepsilon} dz'' g(z'')$$

$$= \int_{-\infty}^{z-\varepsilon} dz' [R_1^2 \delta(z'-z_1) + R_2 R_2' \delta(z'-z_2) + \cdots + R_n R_n' \delta(z'-z_n) + \cdots]$$

$$= \int_{-\infty}^{\infty} dz' H((z-\varepsilon)-z') [R_1^2 \delta(z'-z_1) + R_2 R_2' \delta(z'-z_2) + \cdots + R_n R_n' \delta(z'-z_n) + \cdots]$$

$$= R_1^2 H((z-\varepsilon)-z_1) + R_2 R_2' H((z-\varepsilon)-z_2) + \cdots + R_n R_n' H((z-\varepsilon)-z_n) + \cdots$$

$$= R_1^2 H(z-(z_1+\varepsilon)) + R_2 R_2' H(z-(z_2+\varepsilon)) + \cdots + R_n R_n' H(z-(z_n+\varepsilon)) + \cdots \qquad \text{(A-8)}$$

Now we can prove A-1 gives the $F[b_1(z)]$ in equation (7).

$$F[b_1(z)]$$

$$= \frac{b_1(z)}{[1-(\int_{z-\varepsilon}^{z+\varepsilon} dz' g(z'))^2][1-\int_{-\infty}^{z-\varepsilon} dz' b_1(z') \int_{z'-\varepsilon}^{z'+\varepsilon} dz'' g(z'')]^2}$$

$$= \frac{b_1(z)}{[1-R_1^2 H((z_1+\varepsilon)-z) H(z-(z_1-\varepsilon)) - \cdots]}$$

$$\times \frac{1}{[1-R_1^2 H(z-(z_1+\varepsilon)) - R_2 R_2' H(z-(z_2+\varepsilon)) - \cdots]^2}$$

$$= \frac{R_1}{1-R_1^2} \delta(z-z_1) + \frac{R_2'}{(1-R_1^2)^2(1-R_2^2)} \delta(z-z_2) + \cdots$$

$$+ \frac{R_n'}{(1-R_1^2)^2(1-R_2^2)^2 \cdots (1-R_{n-1}^2)^2(1-R_n^2)} \delta(z-z_n) + \cdots$$

$$= \frac{R_1}{AF_{j=1}} \delta(z-z_1) + \frac{R_2'}{AF_{j=2}} \delta(z-z_2) + \cdots + \frac{R_n'}{AF_{j=n}} \delta(z-z_n) + \cdots \qquad \text{(A-9)}$$

Since $g(z)$ is still unknown, A-2 is to calculate $g(z)$ by $b_1(z)$.

$$g(z) = \frac{b_1(z)}{1-\int_{-\infty}^{z-\varepsilon} dz' b_1(z') \int_{z'-\varepsilon}^{z'+\varepsilon} dz'' g(z'')} \qquad \text{(A-10)}$$

The term $\int_{-\infty}^{z-\varepsilon} dz' b_1(z') \int_{z'-\varepsilon}^{z'+\varepsilon} dz'' g(z'')$ in the denominator:

$$\int_{-\infty}^{z-\varepsilon} dz' b_1(z') \int_{z'-\varepsilon}^{z'+\varepsilon} dz'' g(z'')$$

$$= \int_{-\infty}^{z-\varepsilon} dz' [R_1^2 \delta(z'-z_1) + R_2 R_2' \delta(z'-z_2) + \cdots + R_n R_n' \delta(z'-z_n) + \cdots]$$

$$= \int_{-\infty}^{\infty} dz' H((z-\varepsilon)-z')[R_1^2 \delta(z'-z_1) + R_2 R_2' \delta(z'-z_2) + \cdots + R_n R_n' \delta(z'-z_n) + \cdots]$$

$$= R_1^2 H((z-\varepsilon)-z_1) + R_2 R_2' H((z-\varepsilon)-z_2) + \cdots + R_n R_n' H((z-\varepsilon)-z_n) + \cdots$$

$$= R_1^2 H(z-(z_1+\varepsilon)) + R_2 R_2' H(z-(z_2+\varepsilon)) + \cdots + R_n R_n' H(z-(z_n+\varepsilon)) + \cdots \quad \text{(A-11)}$$

The RHS of A-2,

$$\frac{b_1(z)}{1 - \int_{-\infty}^{z-\varepsilon} dz' b_1(z') \int_{z'-\varepsilon}^{z'+\varepsilon} dz'' g(z'')}$$

$$= R_1 \delta(z-z_1) + \frac{R_2'}{1-R_1 R_1} \delta(z-z_2) + \frac{R_3'}{1-R_1 R_1 - R_2' R_2} \delta(z-z_3) + \cdots$$

$$+ \frac{R_n'}{1-R_1 R_1 - R_2' R_2 - \cdots - R_{n-1}' R_{n-1}} \delta(z-z_n)$$

$$= R_1 \delta(z-z_1) + R_2 \delta(z-z_2) + R_3 \delta(z-z_3) + \cdots + R_n \delta(z-z_n) + \cdots$$

$$= g(z) \quad \text{(A-12)}$$

Thus the second equation is proved.

In the derivation we used: $R_i = \frac{R_i'}{1-R_1 R_1 - R_2' R_2 - \cdots - R_{i-1}' R_{i-1}}$ It can be proved:

$$R_i = \frac{R_i'}{(1-R_1^2)(1-R_2^2)\cdots(1-R_{i-2}^2)(1-R_{i-1}^2)}$$

$$= \frac{R_i'}{(1-R_1^2)(1-R_2^2)\cdots(1-R_{i-2}^2) - (1-R_1^2)(1-R_2^2)\cdots(1-R_{i-2}^2)R_{i-1}^2}$$

$$= \frac{R_i'}{(1-R_1^2)(1-R_2^2)\cdots(1-R_{i-2}^2) - {\color{red}(1-R_1^2)(1-R_2^2)\cdots(1-R_{i-2}^2)R_{i-1}}R_{i-1}}$$

$$= \frac{R_i'}{(1-R_1^2)(1-R_2^2)\cdots(1-R_{i-2}^2) - {\color{red}R_{i-1}'}R_{i-1}}$$

$$= \frac{R_i'}{1-R_1 R_1 - R_2' R_2 - \cdots - R_{i-1}' R_{i-1}} \quad \text{(A-13)}$$

APPENDIX C FOURIER TRANSFORM OF THE DATA FROM THE FREQUENCY-SPACE DOMAIN TO THE FREQUENCY-WAVENUMBER DOMAIN

$$D(x_s, x_g, \omega) = \frac{1}{2\pi} \int_{-\omega/c}^{\omega/c} dk'_s \frac{e^{-ik'_s x_s}}{2iq'_s} R(k'_s, q'_s) e^{ik'_s x_g} e^{2iq'_s z_1} \qquad \text{(A-14)}$$

$$
\begin{aligned}
D(k_s, x_g, \omega) &= \frac{1}{2\pi} \int_{-\infty}^{\infty} dx_s e^{ik_s x_s} \int_{-\omega/c}^{\omega/c} dk'_s \frac{e^{-ik'_s x_s}}{2iq'_s} R(k'_s, q'_s) e^{ik'_s x_g} e^{2iq'_s z_1} \\
&= \frac{1}{2\pi} \int_{-\omega/c}^{\omega/c} \int_{-\infty}^{\infty} dx_s e^{i(k_s - k'_s)x_s} dk'_s \frac{R(k'_s, q'_s) e^{ik'_s x_g} e^{2iq'_s z_1}}{2iq'_s} \\
&= \frac{1}{2\pi} \int_{-\omega/c}^{\omega/c} dk'_s \delta(k_s - k'_s) \frac{R(k'_s, q'_s) e^{ik'_s x_g} e^{2iq'_s z_1}}{2iq'_s} \\
&= \frac{R(k_s, q_s) e^{ik_s x_g} e^{2iq_s z_1}}{4\pi i q_s} (-\omega/c < k_s < \omega/c) \qquad \text{(A-15)}
\end{aligned}
$$

$$
\begin{aligned}
D(k_s, k_g, \omega) &= \int_{-\infty}^{\infty} dx_g e^{-ik_g x_g} \frac{R(k_s, q_s) e^{ik_s x_g} e^{2iq_s z_1}}{4\pi i q_s} (-\omega/c < k_s < \omega/c) \\
&= \delta(k_s - k_g) \frac{R(k_s, q_s) e^{2iq_s z_1}}{4\pi i q_s} (-\omega/c < k_s < \omega/c) \qquad \text{(A-16)}
\end{aligned}
$$

APPENDIX D A 2-REFLECTOR ANALYTIC EXAMPLE FOR THE ISS INTERNAL-MULTIPLE ATTENUATION ALGORITHM IN A 1D PRE-STACK ACOUSTIC MEDIUM

In this section, we discuss a 2-reflector analytic example in a 1D pre-stack acoustic medium. First we calculate the analytic data. Considering a delta source at (x_s, z_s), the wave generated at (x_g, z_g) by this source is (the Green's function):

$$G_0(x_g, z_g, x_s, z_s, \omega) = \frac{1}{2\pi} \int_{-\infty}^{\infty} dk'_s \frac{e^{ik'_s(x_g - x_s)} e^{iq'_s |z_g - z_s|}}{2iq'_s} \qquad \text{(A-17)}$$

Let us set $z_s = 0$ and let z_g be positive, so that we can evaluate the absolute value in the integrand,

$$G_0(x_g, z_g > 0, x_s, z_s = 0, \omega) = \frac{1}{2\pi} \int_{-\infty}^{\infty} dk_s' \frac{e^{-ik_s' x_s}}{2iq_s'} e^{ik_s' x_g + iq_s' z_g}. \qquad \text{(A-18)}$$

Then, for simplicity, the evanescent part is ignored, which means $k_s' < \omega/c$. That does not mean the algorithm can not handle the evanescent part. However, for many cases the evanescent part is small and can be ignored, and the math will be much simpler and easier to understand. Now the Green's function is:

$$G_0(x_g, z_g > 0, x_s, z_s = 0, \omega) = \frac{1}{2\pi} \int_{-\omega/c}^{\omega/c} dk_s' \frac{e^{-ik_s' x_s}}{2iq_s'} e^{ik_s' x_g + iq_s' z_g}. \qquad \text{(A-19)}$$

At this point, G_0 can be regarded as a superposition of plane waves $e^{ik_s' x + iq_s' z}$ with weights $\frac{e^{-ik_s' x_s}}{2iq_s'}$.

For a plane wave $e^{ik_s' x + iq_s' z}$ incident in an acoustic medium, the reflected wavefield is: (Note that it can be calculated by using the forward scattering series, as in Nita et al. (2004))

$$D(k_s', q_s', x_g, z_g = 0) = R(k_s', q_s')e^{ik_s' x_g} e^{2iq_s' z_1}. \qquad \text{(A-20)}$$

Then the total wavefield is (we set $z_g = z_s = 0$):

$$D(x_s, z_s = 0, x_g, z_g = 0, \omega) = \frac{1}{2\pi} \int_{-\omega/c}^{\omega/c} dk_s' \frac{e^{-ik_s' x_s}}{2iq_s'} D(k_s', q_s', x_g, z_g = 0). \qquad \text{(A-21)}$$

Now we get the data at one receiver $(x_g, 0)$ from one delta source $(x_s, 0)$ and rewrite it as:

$$D(x_s, x_g, \omega) = \frac{1}{2\pi} \int_{-\omega/c}^{\omega/c} dk_s' \frac{e^{-ik_s' x_s}}{2iq_s'} R(k_s', q_s')e^{ik_s' x_g} e^{2iq_s' z_1} \qquad \text{(A-22)}$$
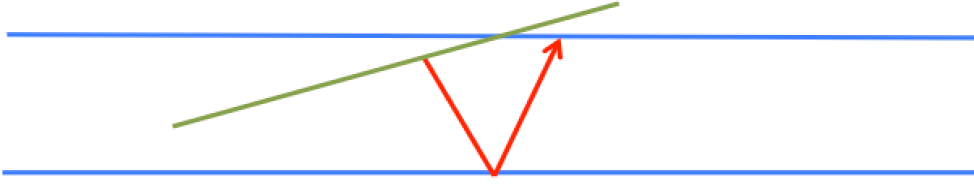
Figure 3: reflection of one plane wave component

This is in the frequency-space domain, whereas the attenuation algorithm works in the frequency-wavenumber domain. After Fourier transforming over the source and receivers, we convert the data to the frequency-wavenumber domain[*].

$$D(k_s, k_g, \omega) = \delta(k_s - k_g)\frac{R(k_s, q_s)e^{2iq_s z_1}}{4\pi i q_s}(-\omega/c < k_s < \omega/c) \qquad \text{(A-23)}$$

Now we define $b_1(k_s, k_g, \omega)$ as (in the following discussion, we assume that $-\omega/c < k_s < \omega/c$):

$$
\begin{aligned}
b_1(k_s, k_g, \omega) &= -2iq_s D(k_s, k_g, \omega) \\
&= -\frac{1}{2\pi}\delta(k_s - k_g)R(k_s, q_s)e^{2iq_s z_1}.
\end{aligned}
\qquad \text{(A-24)}
$$

Then, $b_1(k_s, k_g, \omega)$ and the attenuation algorithm prediction $b_3(k_s, k_g, \omega)$ are related by the 2D internal-multiple attenuation algorithm:

$$
\begin{aligned}
b_3(k_g, k_s, \omega) &= \int_{-\infty}^{\infty}\int_{-\infty}^{\infty} dk_1 dk_2 \int_{-\infty}^{\infty} dz e^{i(q_g+q_1)z}b_1(k_g, k_1, z)\int_{-\infty}^{z} dz' e^{i(-q_1-q_2)z'}b_1(k_1, k_2, z') \\
&\quad \times \int_{z'}^{\infty} dz'' e^{i(q_2+q_s)z''}b_1(k_2, k_s, z'')
\end{aligned}
$$

_____

[*]See appendix C for derivation

Next with the definition of $b_1(k_s, 2q_s)$ and its prediction $b_3(k_s, 2q_s)$ for 1D pre-stack data, we have:

$$b_1(k_s, k_g, \omega) = -\frac{1}{2\pi}\delta(k_s - k_g)b_1(k_s, 2q_s) \tag{A-25}$$

$$b_3(k_g, k_s, q_g + q_s) = -\frac{1}{(2\pi)^3}\delta(k_g - k_s)b_3(k_s, 2q_s). \tag{A-26}$$

Then, $b_1(k_s, 2q_s)$ and $b_3(k_s, 2q_s)$ are related by the 1D pre-stack algorithm:

$$b_3(k_s, 2q_s) = \int_{-\infty}^{\infty} dz e^{2iq_s z} b_1(k_s, z) \int_{-\infty}^{z} dz' e^{-2iq_s z'} b_1(k_s, z') \int_{z'}^{\infty} dz'' e^{2iq_s z''} b_1(k_s, z'') \tag{A-27}$$

Ignoring the subscript s, we have

$$b_3(k, 2q) = \int_{-\infty}^{\infty} dz e^{2iqz} b_1(k, z) \int_{-\infty}^{z} dz' e^{-2iqz'} b_1(k, z') \int_{z'}^{\infty} dz'' e^{2iqz''} b_1(k, z''). \tag{A-28}$$

In the equation, for the first primary, we have

$$b_1(k, 2q) = R(k, q)e^{2iqz_1}, \tag{A-29}$$

and $b_1(k, z)$ is the Fourier transform of $b_1(k, 2q)$ from 2q to z.

We can also get the reflection data from the second reflector, and we can obtain a first-order internal multiple as shown in Figure 4

Now, b_1 can be written as,

$$b_1(k_1, 2q_1) = R_1(k_1, q_1)e^{2iq_1 z_1}$$

$$+ T_{01} R_2(k_2, q_2) T_{10} e^{2iq_1 z_1} e^{2iq_2(z_2 - z_1)}$$

$$- T_{01} R_2 R_1 R_2 T_{10} e^{2iq_1 z_1} e^{4iq_2(z_2 - z_1)} \tag{A-30}$$

Here, q_1 and q_2 are vertical wavenumbers at each layer, and q_2 is a function of q_1. To Fourier transform from q_1 to z, first we need to substitute q_2 with q_1.
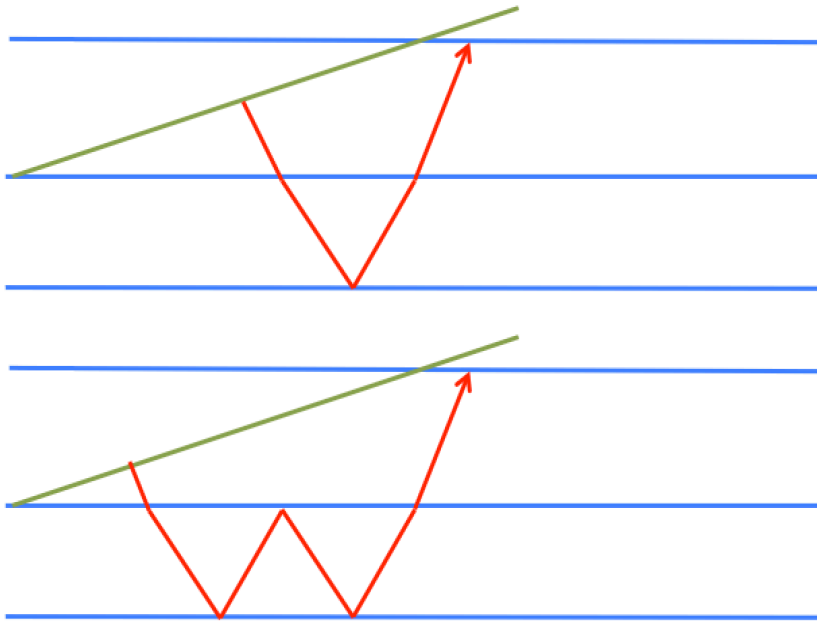
Figure 4: reflection of one plane wave component

Using the relation,

$$q_1^2 + k_1^2 = (\frac{\omega}{c_1})^2 \tag{A-31}$$

$$q_2^2 + k_2^2 = (\frac{\omega}{c_2})^2 \tag{A-32}$$

$$k_1 = k_2, \tag{A-33}$$

we can express q_2 in q_1 and k_1:

$$
\begin{aligned}
q_2 &= \sqrt{(\frac{c_1^2}{c_2^2}-1)k_1^2+\frac{c_1^2}{c_2^2}q_1^2} \\[2mm]
&= \frac{c_1}{c_2}q_1+[\sqrt{(\frac{c_1^2}{c_2^2}-1)k_1^2+\frac{c_1^2}{c_2^2}q_1^2}-\frac{c_1}{c_2}q_1] \\[2mm]
&= \frac{c_1}{c_2}q_1+\frac{(\frac{c_1^2}{c_2^2}-1)k_1^2}{\sqrt{(\frac{c_1^2}{c_2^2}-1)k_1^2+\frac{c_1^2}{c_2^2}q_1^2}+\frac{c_1}{c_2}q_1} \\[2mm]
&= \frac{c_1}{c_2}q_1+S(k_1,q_1) \qquad\qquad\qquad\qquad\qquad \text{(A-34)}
\end{aligned}
$$

Now we substitute q_2 with q_1:

$$
\begin{aligned}
b_1(k_1,2q_1) &= R_1(k_1,q_1)e^{2iq_1z_1} \\[2mm]
&\quad +R_2'(k_1,q_1)e^{2i(z_2-z_1)S(k_1,q_1)}e^{2iq_1(z_1+\frac{c_1}{c_2}(z_2-z_1))} \\[2mm]
&\quad -R_{212}'(k_1,q_1)e^{4i(z_2-z_1)S(k_1,q_1)}e^{2iq_1(z_1+\frac{2c_1}{c_2}(z_2-z_1))} \\[2mm]
&= R_1(k_1,q_1)e^{2iq_1z_1} \\[2mm]
&\quad +R_2'(k_1,q_1)e^{2i(z_2-z_1)S(k_1,q_1)}e^{2iq_1z_2'} \\[2mm]
&\quad -R_{212}'(k_1,q_1)e^{4i(z_2-z_1)S(k_1,q_1)}e^{2iq_1(2z_2'-z_1)} \qquad\qquad \text{(A-35)}
\end{aligned}
$$

The predicted internal multiple should be:

$$
b_3(k_1,2q_1) = R_2'(k_1,q_1)R_1(k_1,q_1)R_2'(k_1,q_1)e^{4i(z_2-z_1)S(k_1,q_1)}e^{2iq_1(2z_2'-z_1)} \qquad \text{(A-36)}
$$

Comparing the predicted amplitude of the internal multiple with the actual amplitude of the internal multiple, we have:

$$
\begin{aligned}
R_{212}'(k_1,q_1) &= T_{01}R_2R_1R_2T_{10} \\[2mm]
&= \frac{R_2'(k_2,q_2)R_1(k_1,q_1)R_2'(k_2,q_2)}{T_{01}(k_1,q_1)T_{10}(k_1,q_1)} \qquad\qquad \text{(A-37)}
\end{aligned}
$$

We can see that they differed by a factor $T_{01}(k_1, q_1)T_{10}(k_1, q_1)$. That is the attenuation factor for first-order internal multiples generated by the shallowest reflector in a 1D pre-stack acoustic medium.

REFERENCES

Araújo, F. V., A. B. Weglein, P. M. Carvalho, and R. H. Stolt, 1994, Inverse scattering series for multiple attenuation: An example with surface and internal multiples: SEG Technical Program Expanded Abstracts, 1039–1041.

Carvalho, P. M., 1992, Free-surface multiple reflection elimination method based on non-linear inversion of seismic data: PhD thesis, Universidade Federal da Bahia.

Carvalho, P. M., A. B. Weglein, and R. H. Stolt, 1992, Nonlinear inverse scattering for multiple suppression: Application to real data. part i: 62nd Annual International Meeting, SEG, Expanded Abstracts, 1093–1095.

Fu, Q., Y. Zou, J. Wu, and A. B. Weglein, 2018, Analysis of the inverse scattering series (iss) internal multiple attenuation and elimination algorithms as effective tool box choices for absorptive and dispersive media with interfering events: Submitted to SEG Technical Program Expanded Abstracts.

H. Liang, C. M., and A. B. Weglein, 2012, A further general modification of the leading order iss attenuator of first-order internal multiples to accommodate primaries and internal multiples when an arbitrary number of reflectors generate the data: theory, development, and examples: Mission Oriented Seismic Research Program Annual Report, 148–165.

Herrera, Chao Ma, H. L. P. T., and A. B. Weglein, 2012, Progressing amplitude issues for testing 1d analytic data in leading order internal multiple algorithms: Mission Oriented Seismic Research Program Annual Report, 167–188.

Innanen, K. A., 2017, Time- and offset-domain internal multiple prediction with nonstationary parameters: GEOPHYSICS, **82**, v105–v166.

Ma, C., Q. Fu, and A. B. Weglein, 2018, Analysis, testing and comparison of the inverse scattering series (iss) free-surface multiple-elimination (fsme) algorithm, and the industry-

standard srme plus energy minimization adaptive subtraction: Geophysics.

Ma, C., H. Liang, and A. B. Weglein, 2012, Modifying the leading order iss attenuator of first-order internal multiples to accommodate primaries and internal multiples: fundamental concept andtheory, development, and examples exemplified when three reflectors generatethe data: Mission Oriented Seismic Research Program Annual Report, 133–147.

Ma, C., and A. B. Weglein, 2014, Including higher-order inverse scattering series (iss) terms to address a serious shortcoming/problem of the iss internal-multiple attenuator: exemplifying the problem and its resolution: SEG Technical Program Expanded Abstracts.

Mayhan, J. D., and A. B. Weglein, 2013, First application of Green's theorem-derived source and receiver deghosting on deep-water Gulf of Mexico synthetic (SEAM) and field data: Geophysics, **78**, WA77–WA89.

Nita, B. G., K. H. Matson, and A. B. Weglein, 2004, Forward scattering series and seismic events: Far field approximations, critical and postcritical events: SIAM Journal of Applied Mathematics, **64**, 2167–2185.

Ramírez, A. C., 2007, 1.-inverse scattering subseries for removal of internal multiples and depth imaging primaries; 2.-green's theorem as the foundation of interferometry and guiding new practical methods and applications: PhD thesis, University of Houston.

Shen, Y., and A. B. Weglein, 2017, Impact of the shape of the acquisition surface on the effectiveness of the iss internal multiple attenuation and elimination algorithms: Analyzing the problem and providing a response to the challenge: SEG Technical Program Expanded Abstracts.

Stolt, R. H., and A. B. Weglein, 2013, Seismic imaging and inversion: Cambridge University Press, **1**.

Wang, Y., 2003, Multiple subtraction using an expanded multichannel matching filter: Geo-

physics, **68**, 346–354.

Weglein, A. B., 2014, Multiple attenuation: The status and a strategy that identifies and addresses current challenges.

Weglein, A. B., F. V. Araújo, P. M. Carvalho, R. H. Stolt, K. H. Matson, R. T. Coates, D. Corrigan, D. J. Foster, S. A. Shaw, and H. Zhang, 2003, Inverse scattering series and seismic exploration: Inverse Problems, R27–R83.

Weglein, A. B., F. A. Gasparotto, P. M. Carvalho, and R. H. Stolt, 1997, An inverse-scattering series method for attenuating multiples in seismic reflection data: Geophysics, **62**, 1975–1989.

Weglein, A. B., and K. H. Matson, 1998, Inverse scattering internal multiple attenuation: An analytic example and subevent interpretation: SPIE Conference on Mathematical Methods in Geophysical Imaging, 108–117.

Weglein, A. B., S. A. Shaw, K. H. Matson, J. L. Sheiman, R. H. Solt, T. H. Tan, A. Osen, G. P. Correa, K. A. Innanen, Z. Guo, and J. Zhang, 2002, New approaches to deghosting towed-streamer and ocean-bottom pressure measurements: 72nd Annual International Meeting, SEG, Expanded Abstracts, 1016–1019.

Wu, J., and A. B. Weglein, 2016, Green's theorem-based onshore preprocessing: A reduced data requirement assuming a vacuum/earth model for the air/earth interface and the evaluation of the usefulness of that assumption: SEG Technical Program Expanded Abstracts.

Zhang, J., 2007, Wave theory based data preparation for inverse scattering multiple removal, depth imaging and parameter estimation: analysis and numerical tests of Green's theorem deghosting theory: PhD thesis, University of Houston.

Zhang, Z., and A. B. Weglein, 2016, 2d green?s theorem receiver deghosting in the (x-omega)

domain using a depth-variable cable towards on-shore and ocean-bottom application with variable topography: SEG Technical Program Expanded Abstracts.

Zou, Y., C. Ma, and A. B. Weglein, 2016, The first inverse-scattering-series internal multiple elimination method for a multi-dimensional subsurface: MOSRP annual report.

Zou, Y., and A. B. Weglein, 2014, An internal-multiple elimination algorithm for all reflectors for 1d earth part i: Strengths and limitations: Journal of Seismic Exploration.

LIST OF FIGURES

the data to predict a first-order internal multiple generated by the second reflector

15   a diagram for the attenuation algorithm where three subevents that satisfy a higher-lower-higher relationship is combined to predict an internal multiple.

16   a diagram for a higher order term in the elimination algorithm. There are two more orders of data in the middle compared to the attenuation algorithm. These two more orders of data provides two more orders of $R_1(R_1^2)$ in the prediction.

17   a diagram for another higher order term in the elimination algorithm. There are four more orders of data in the middle compared to the attenuation algorithm. These two more orders of data provides four more orders of $R_1(R_1^4)$ in the prediction.

18   2D Model

19   Zero offset traces of data

20   Zero offset traces after ISS internal-multiple attenuation and energy minimization adaptive subtraction

21   Zero offset traces after ISS internal-multiple elimination

22   1D acoustic model that mimics the 2D acoustic model.

23   Synthetic data set generated based on model shown in Figure 22 using reflectivity method.

24   predictions of internal multiples by the ISS IMA

25   predictions of internal multiples by the ISS IME

26   wiggle plots of P_3 and IM_{212} in the data

27   wiggle plots of P_3 in the data

28   wiggle plots of IM_{212} in the data

29   result after directly subtracting the prediction result of ISS IMA from the data

30   result of ISS IMA plus energy-minimization adaptive subtraction

31   result after directly subtracting the prediction result of ISS IME from the data

$F[b_1(z)] \leftarrow$ ⌐ $b_1(z)$

⌐ $partial\ R'$ ⌐ $b_1(z)$

$AF \leftarrow T \leftarrow all\ R \leftarrow$

$partial\ R$ $g(z) \leftarrow b_1(z)$
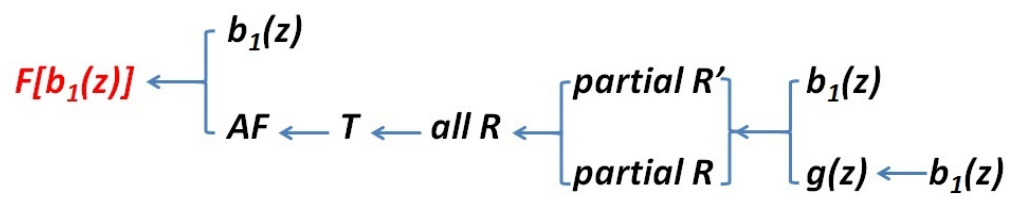
Figure 5:

Zou, Ma & Weglein – GEO-ISS-IME
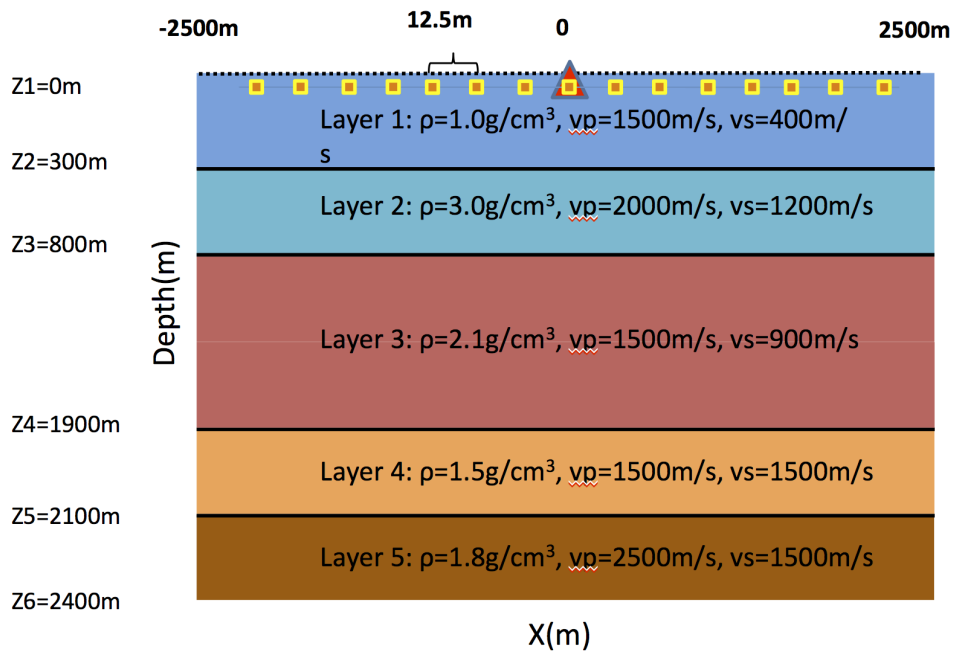
Figure 6: model

Zou, Ma & Weglein – GEO-ISS-IME
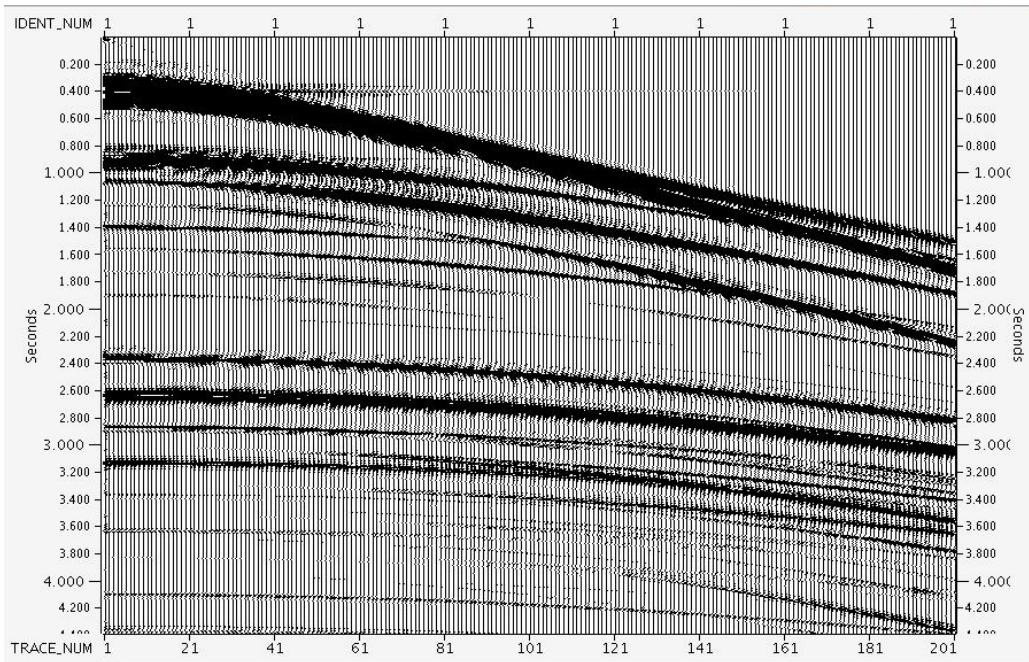
Figure 7: PP data

Zou, Ma & Weglein – GEO-ISS-IME
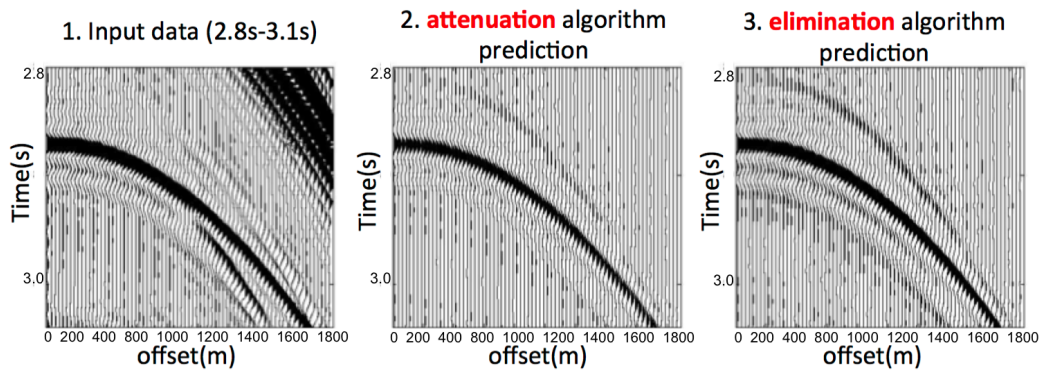
Figure 8: A section of the input data and prediction. Left: input data. Middle: attenuation algorithm prediction. Right:elimination algorithm prediction.

Zou, Ma & Weglein – GEO-ISS-IME
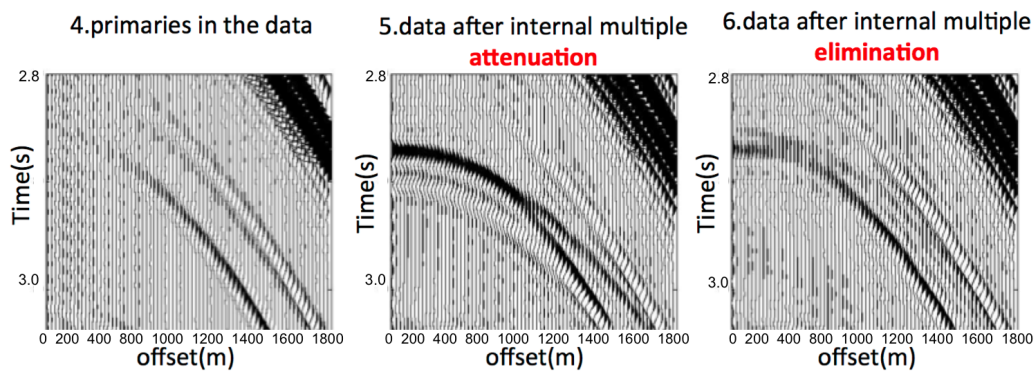
Figure 9: Left: primaries in the input data. Middle: data after internal multiples being attenuated. Right:data after internal multiples being eliminated.

Zou, Ma & Weglein – GEO-ISS-IME

Algorithms	Requirements	Properties
SRME	no subsurface information needs adaptive subtraction	predicts approximate amplitude and time of free-surface multiples
ISS free-surface multiple elimination algorithm	no subsurface information	predicts exact time and amplitude of free-surface multiples, model-type independent

Algorithms	Requirements	Properties
the internal multiple removal methods from DELFT	needs the information down to and include the internal multiple generator	predicts approximate amplitude and time of free-surface multiples
ISS internal multiple attenuation algorithm	no subsurface information	predicts exact time and approximate amplitude of internal multiples, model-type independent

Figure 10:

Zou, Ma & Weglein – GEO-ISS-IME
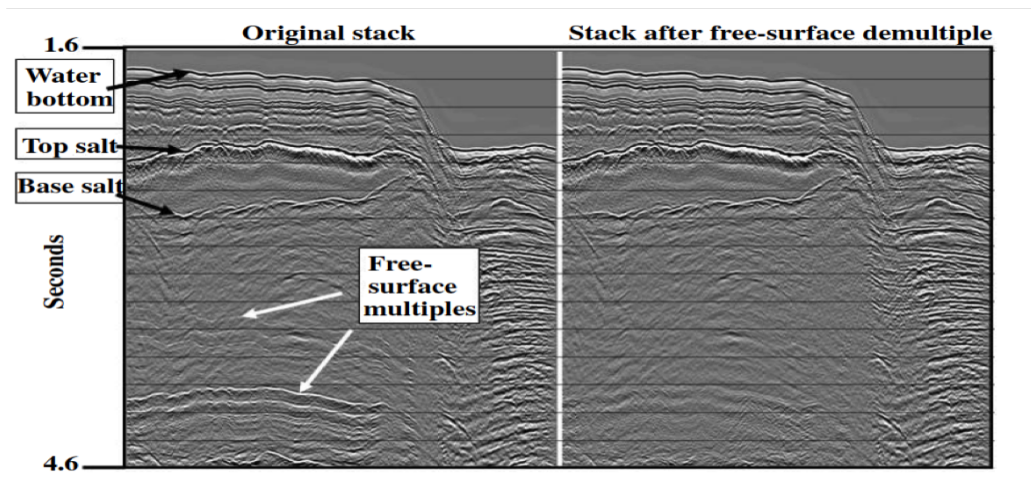
Figure 11: The left panel is a stack of a field data set from the Gulf of Mexico. The right panel is the result of inverse-scattering free-surface multiple removal. Data are courtesy of WesternGeco. Matson et al. (2000),Weglein et al.(2003)

Zou, Ma & Weglein – GEO-ISS-IME
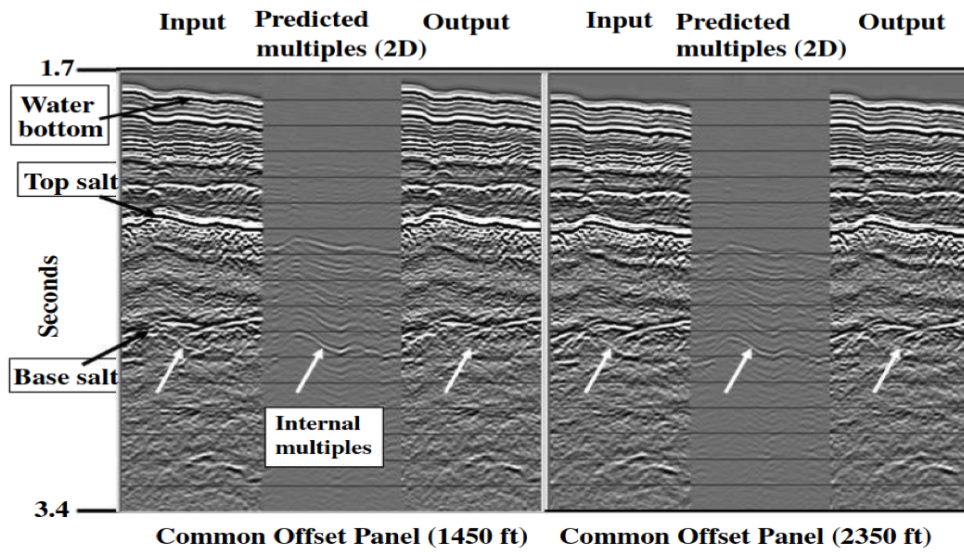
Figure 12: An example of inverse-scattering internal multiple attenuation from the Gulf of Mexico. Data are courtesy of WesternGeco. Matson et al. (2000),Weglein et al.(2003)

Zou, Ma & Weglein – GEO-ISS-IME
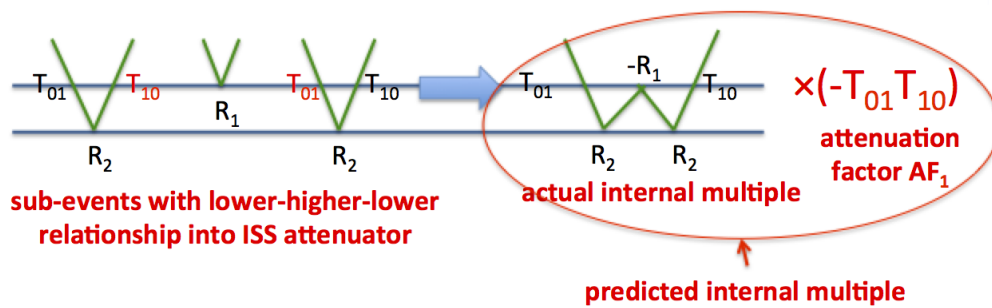
Figure 13: ISS internal-multiple attenuation algorithm automatically uses three primaries

in the data to predict a first-order internal multiple generated by the shallowest reflector

Zou, Ma & Weglein – GEO-ISS-IME
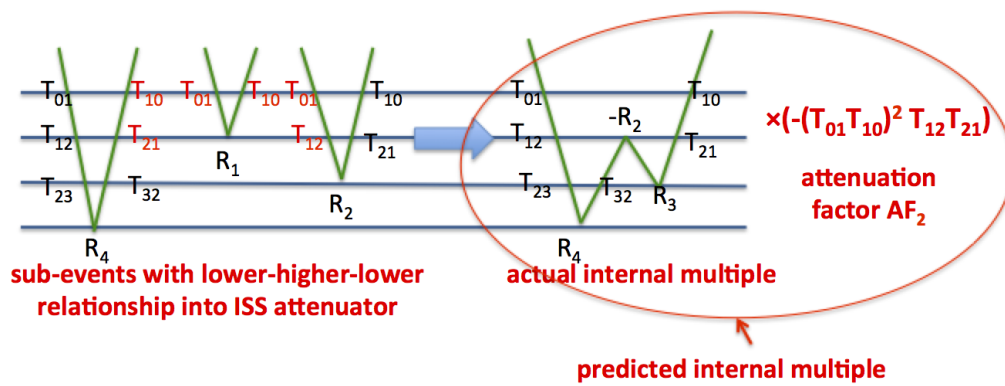
Figure 14: ISS internal-multiple attenuation algorithm automatically uses three primaries in the data to predict a first-order internal multiple generated by the second reflector

Zou, Ma & Weglein – GEO-ISS-IME
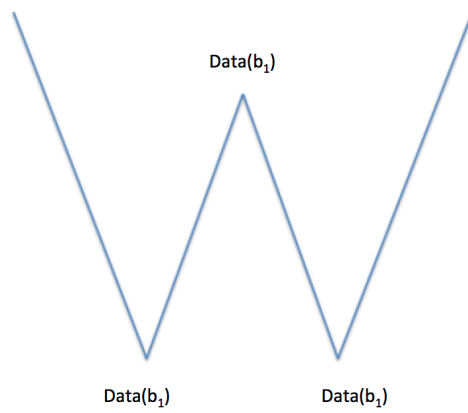
Figure 15: a diagram for the attenuation algorithm where three subevents that satisfy a higher-lower-higher relationship is combined to predict an internal multiple.

Zou, Ma & Weglein – GEO-ISS-IME
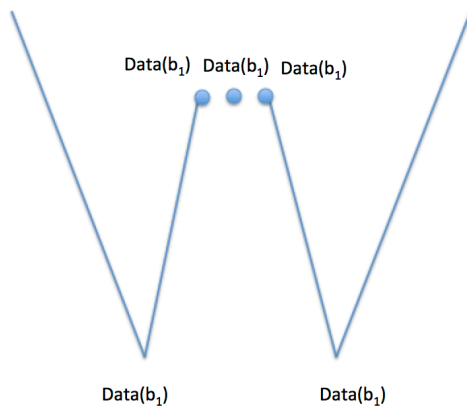
Figure 16: a diagram for a higher order term in the elimination algorithm. There are two more orders of data in the middle compared to the attenuation algorithm. These two more orders of data provides two more orders of $R_1(R_1^2)$ in the prediction.

Zou, Ma & Weglein – GEO-ISS-IME
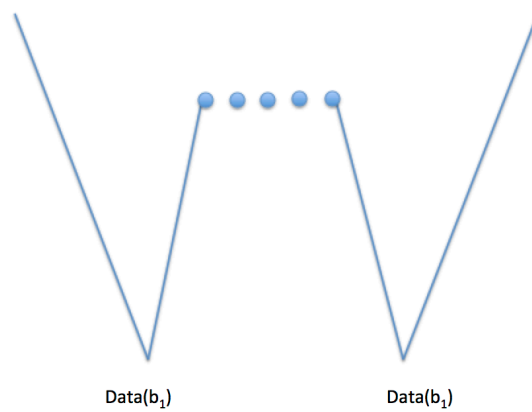
Figure 17: a diagram for another higher order term in the elimination algorithm. There are four more orders of data in the middle compared to the attenuation algorithm. These two more orders of data provides four more orders of $R_1(R_1^4)$ in the prediction.

Zou, Ma & Weglein – GEO-ISS-IME

2D model

127 sources,127 receivers, 2seconds
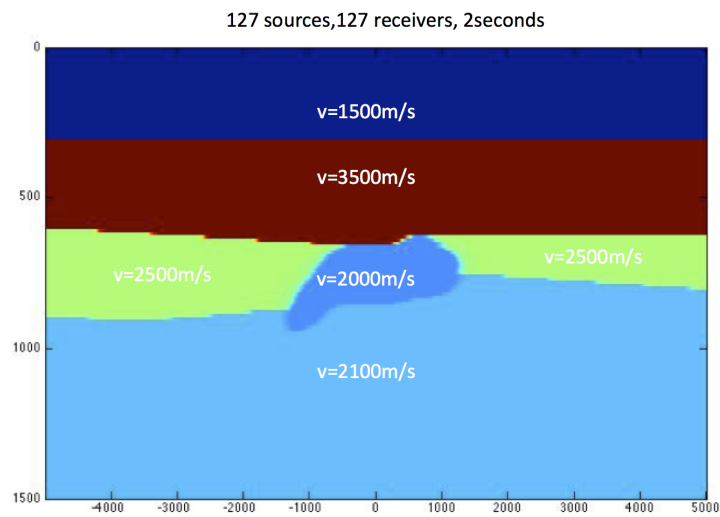
Figure 18: 2D Model

Zou, Ma & Weglein – GEO-ISS-IME
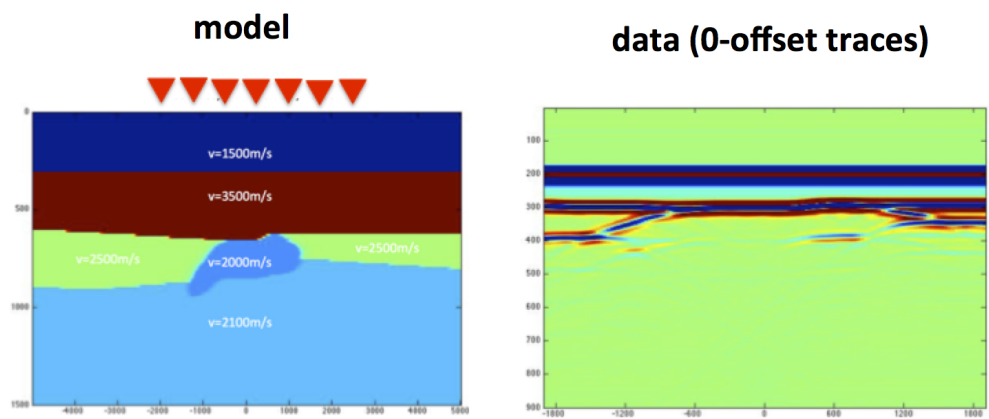
Figure 19: Zero offset traces of data

Zou, Ma & Weglein – GEO-ISS-IME
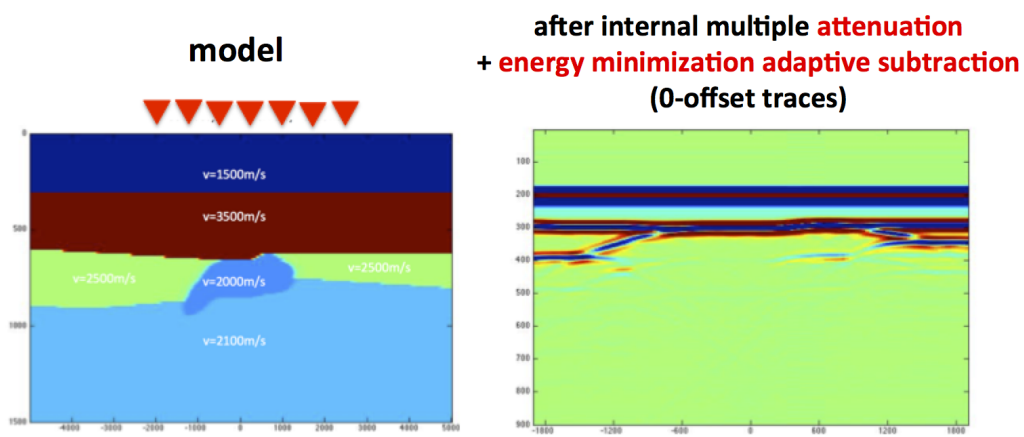
Figure 20: Zero offset traces after ISS internal-multiple attenuation and energy minimization adaptive subtraction

Zou, Ma & Weglein – GEO-ISS-IME
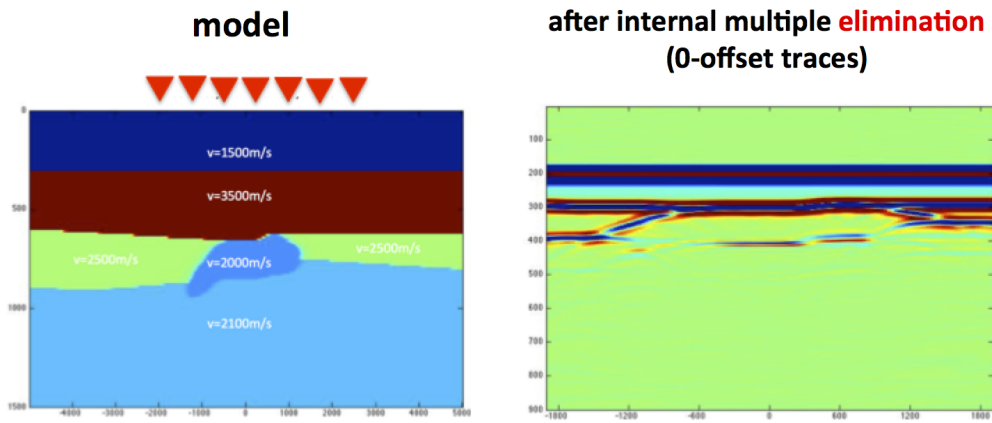
Figure 21: Zero offset traces after ISS internal-multiple elimination

Zou, Ma & Weglein – GEO-ISS-IME

Figure 22: 1D acoustic model that mimics the 2D acoustic model.

Zou, Ma & Weglein – GEO-ISS-IME
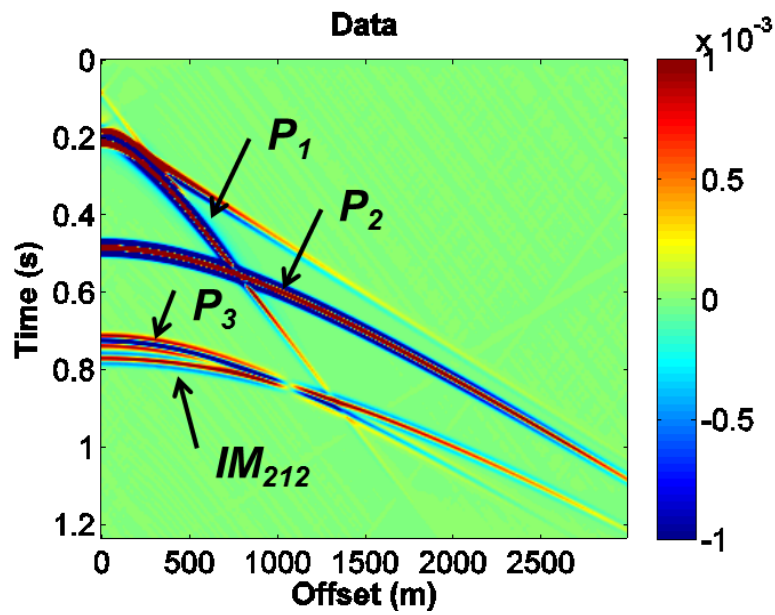
Figure 23: Synthetic data set generated based on model shown in Figure 22 using reflectivity method.

Zou, Ma & Weglein – GEO-ISS-IME
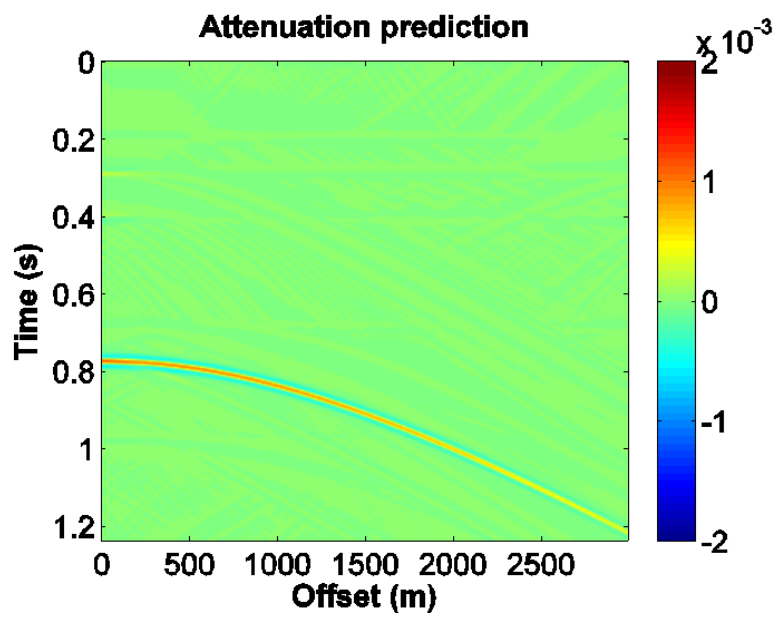
Figure 24: predictions of internal multiples by the ISS IMA

Zou, Ma & Weglein – GEO-ISS-IME
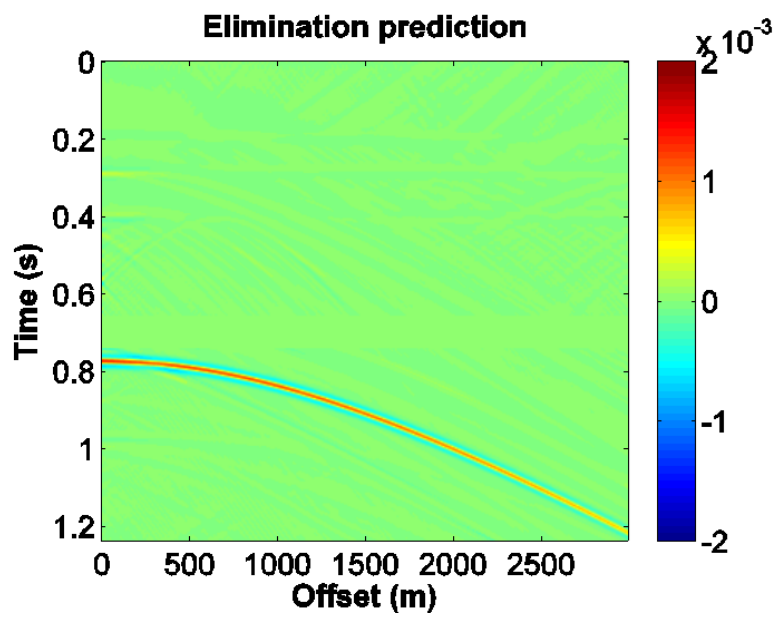
Figure 25: predictions of internal multiples by the ISS IME

Zou, Ma & Weglein – GEO-ISS-IME
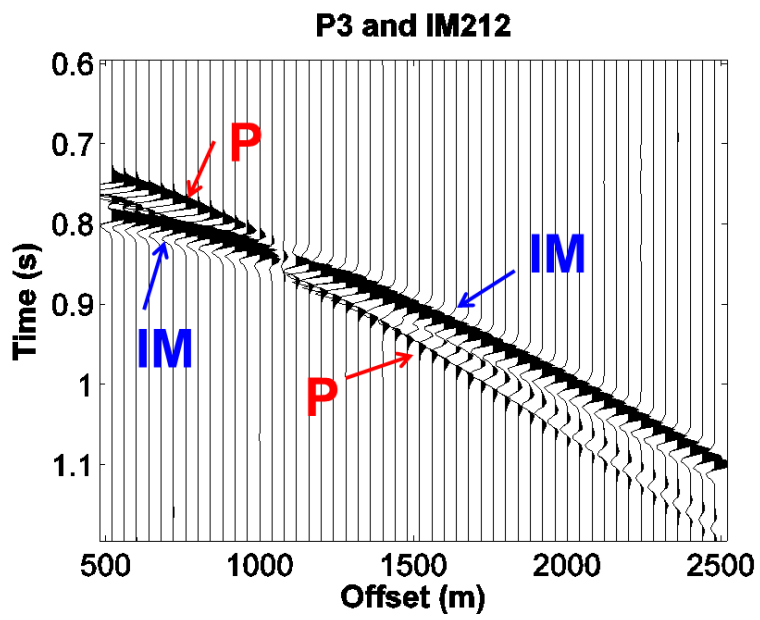
Figure 26: wiggle plots of P_3 and IM_{212} in the data

Zou, Ma & Weglein – GEO-ISS-IME
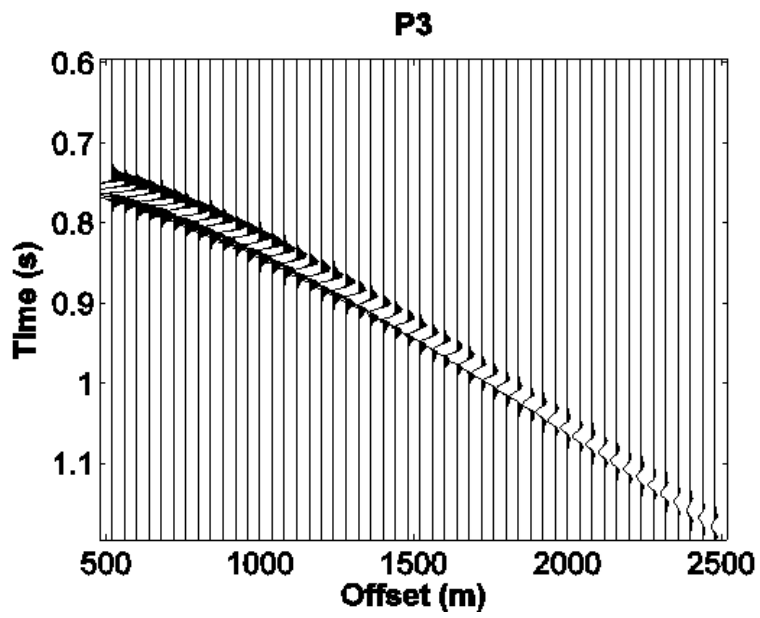
Figure 27: wiggle plots of P_3 in the data

Zou, Ma & Weglein – GEO-ISS-IME
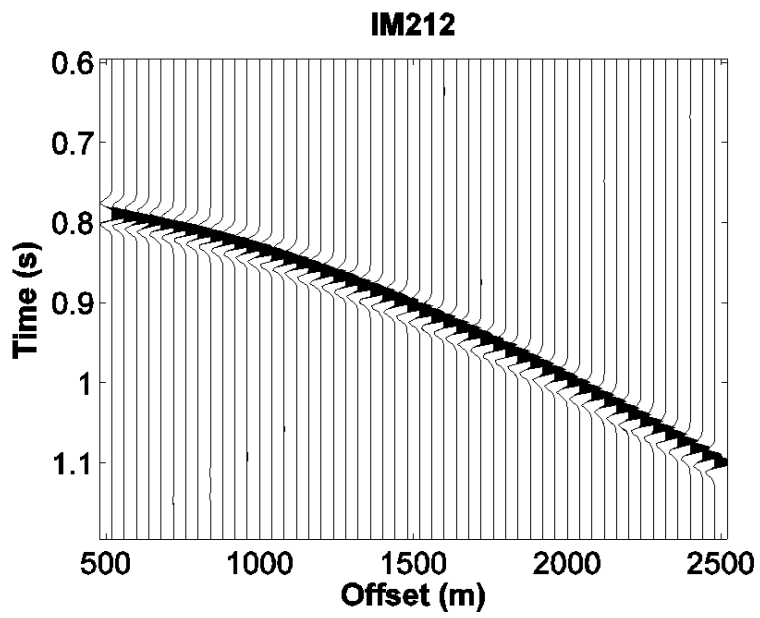
Figure 28: wiggle plots of IM_{212} in the data

Zou, Ma & Weglein – GEO-ISS-IME
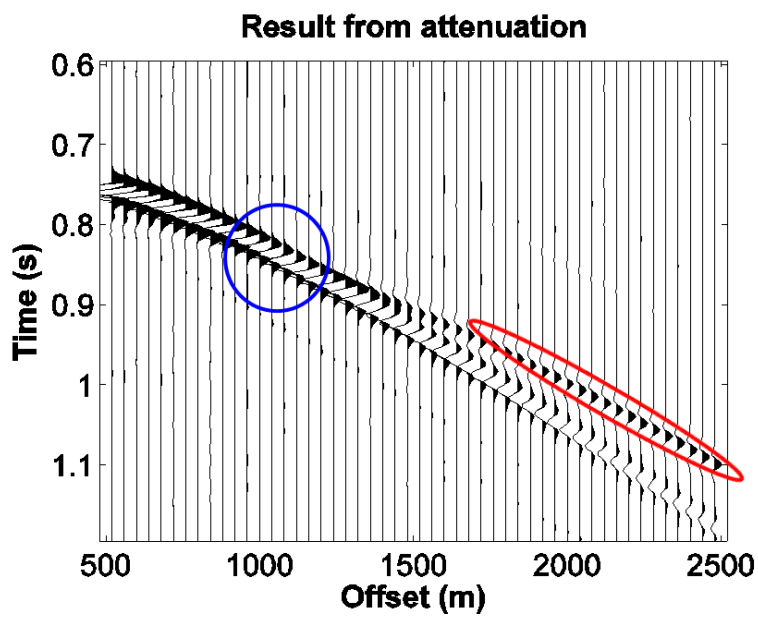
Figure 29: result after directly subtracting the prediction result of ISS IMA from the data

Zou, Ma & Weglein – GEO-ISS-IME
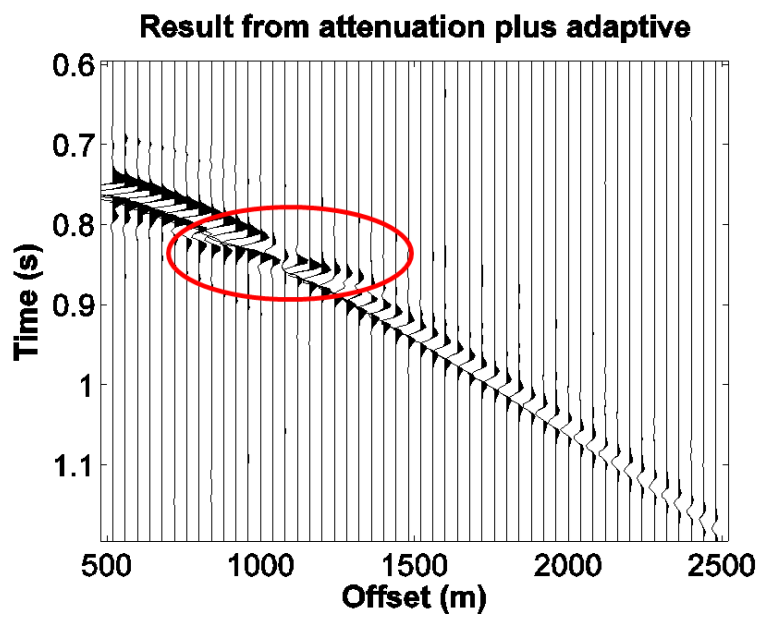
Figure 30: result of ISS IMA plus energy-minimization adaptive subtraction

Zou, Ma & Weglein – GEO-ISS-IME

Result from elimination
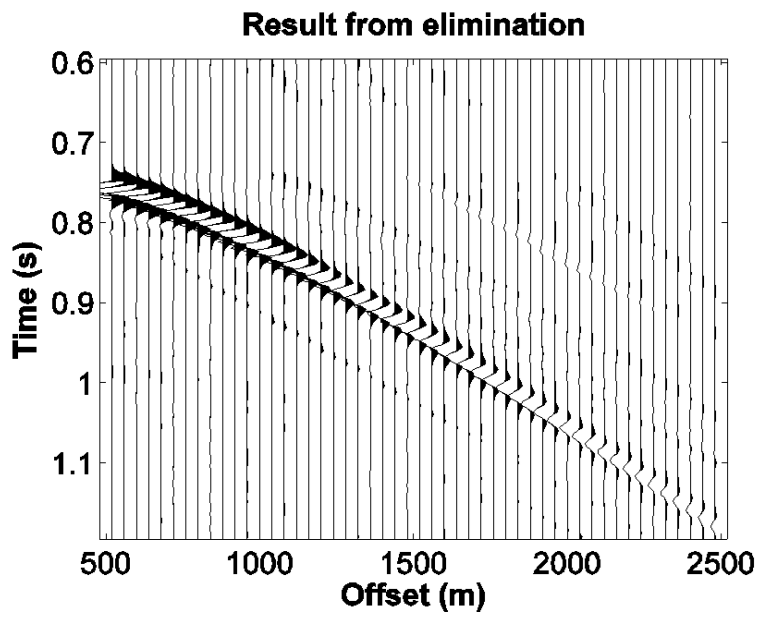
Figure 31: result after directly subtracting the prediction result of ISS IME from the data

Zou, Ma & Weglein – GEO-ISS-IME